# NEUTRON STAR RADIUS FROM GRAVITATIONAL-WAVE OBSERVATIONS

B.S. Sathyaprakash

Bert Elsbach Professor of Physics, Penn State University, USA

and Professor of Physics, Cardiff University, UK

DAWN III Workshop, Syracuse, July 6-7, 2017

# Measuring Neutron Star Equation of State

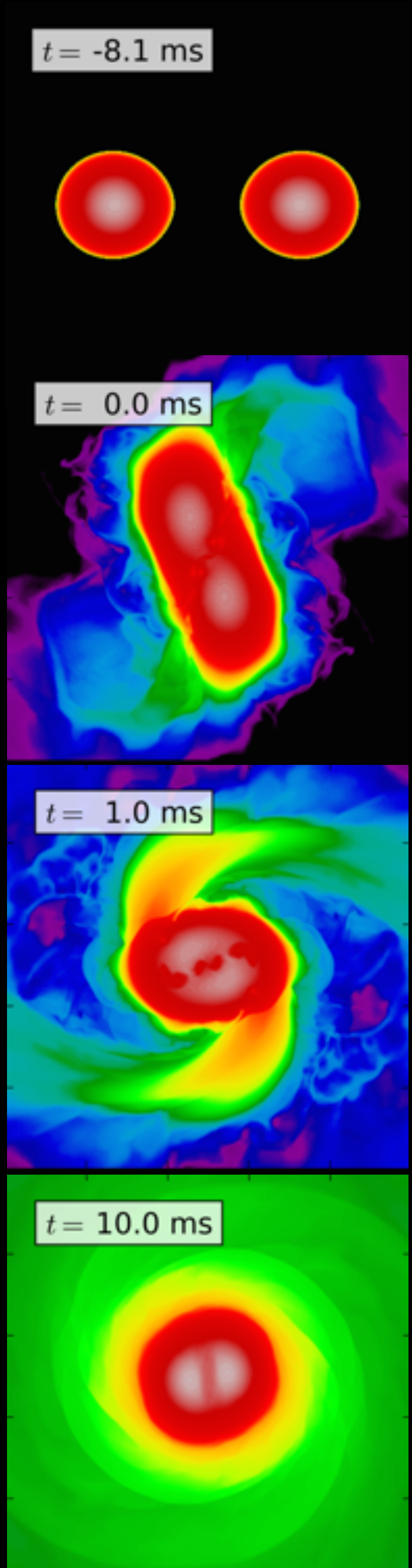


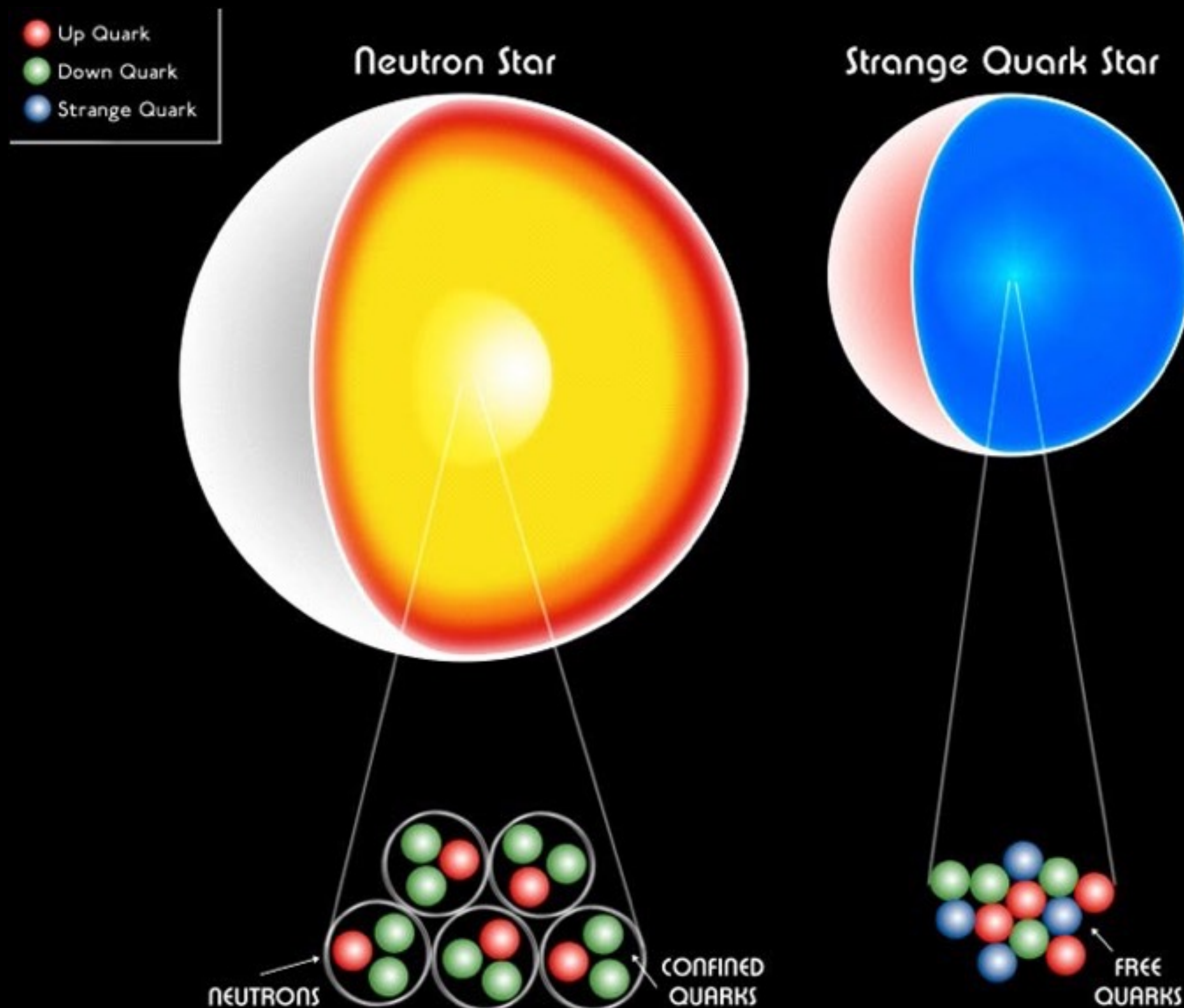


Densities ~ 4 x$10^{17}$ kg/m$^3$

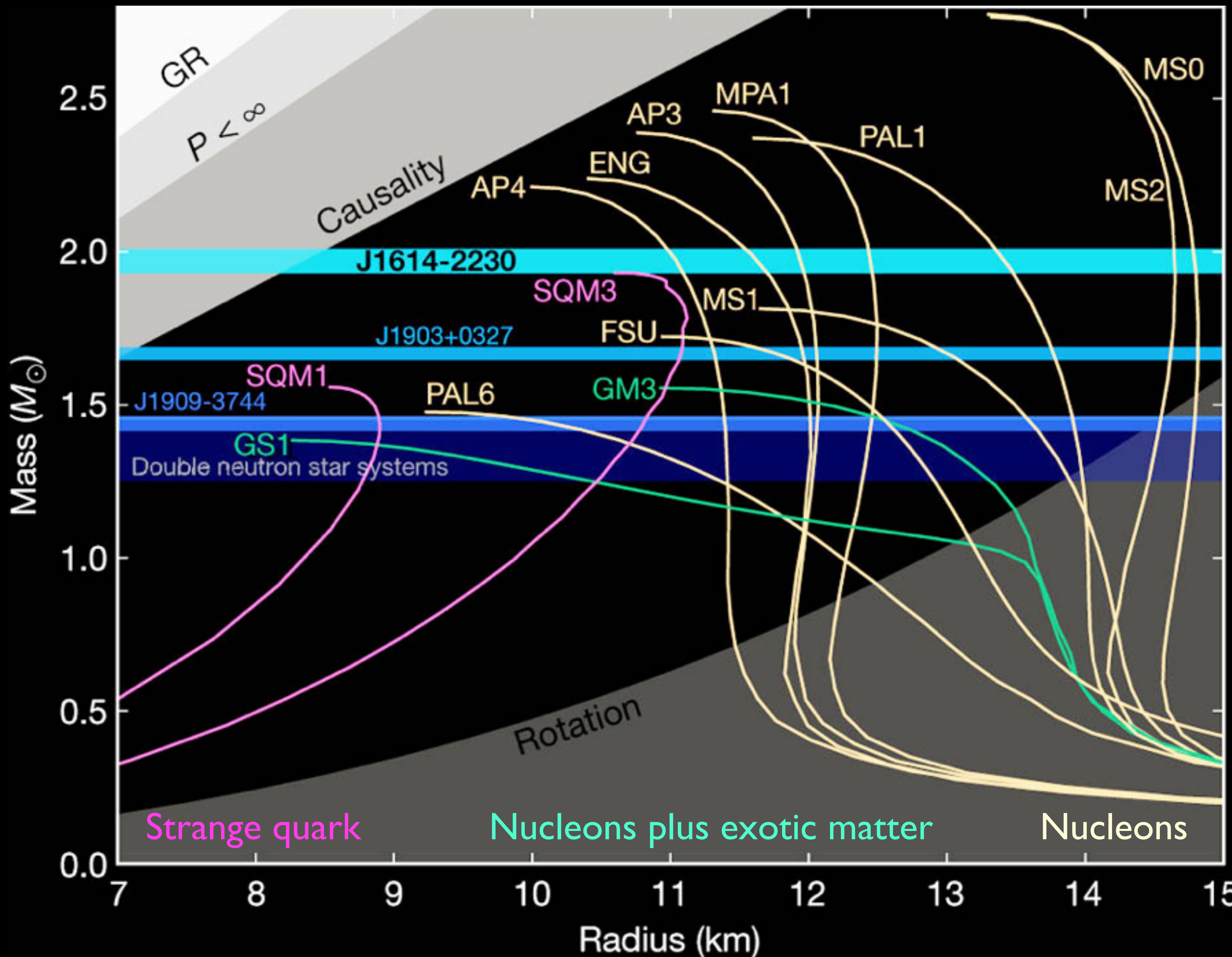


Demorest+, Nature 2010

# LIGO SENSITIVITY DURING FIRST OBSERVING RUN (O1)

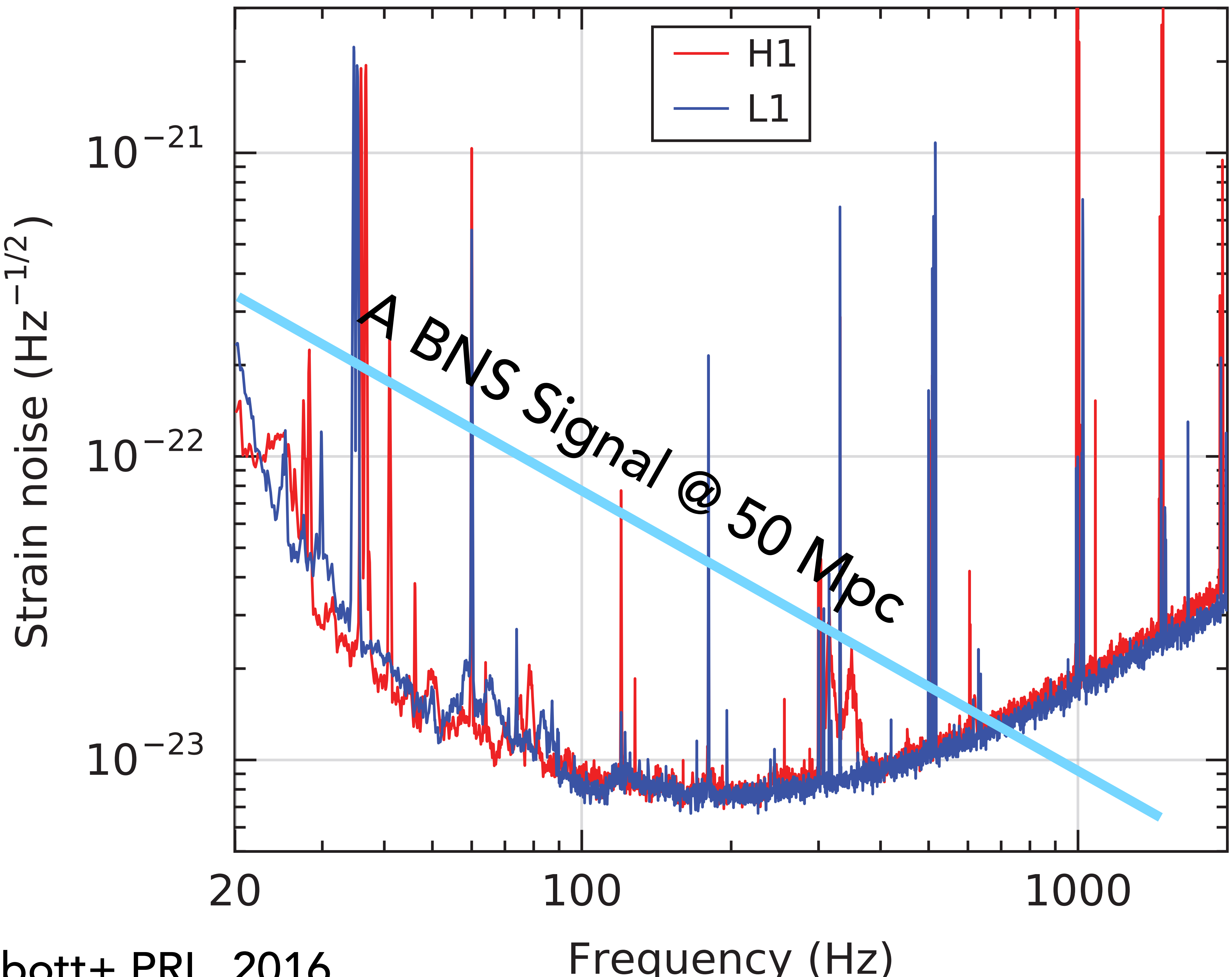


Abbott+ PRL, 2016

# EXPECTED NS-NS MERGER RATES

- observed short GRB rate ~ 0.1 to 10 $yr^{-1}$ $Gpc^{-3}$
- we won't observe all GRBs because
  - most GRB satellites are not sensitive to the whole sky and gamma emission is not expected to be isotropic
- comoving volume rate depends on the beaming angle
  - smaller the beaming angle, less likely we will observe them and so greater the intrinsic rate
- half beaming angle of [5°  ,90°] gives a comoving volume rate of [0.1, 1,000] $yr^{-1}$ $Gpc^{-3}$
  - implies a detection rate of ~ 0.03-30 $yr^{-1}$ at LIGO-Virgo design sensitivity

# BINARY NEUTRON STAR MERGER

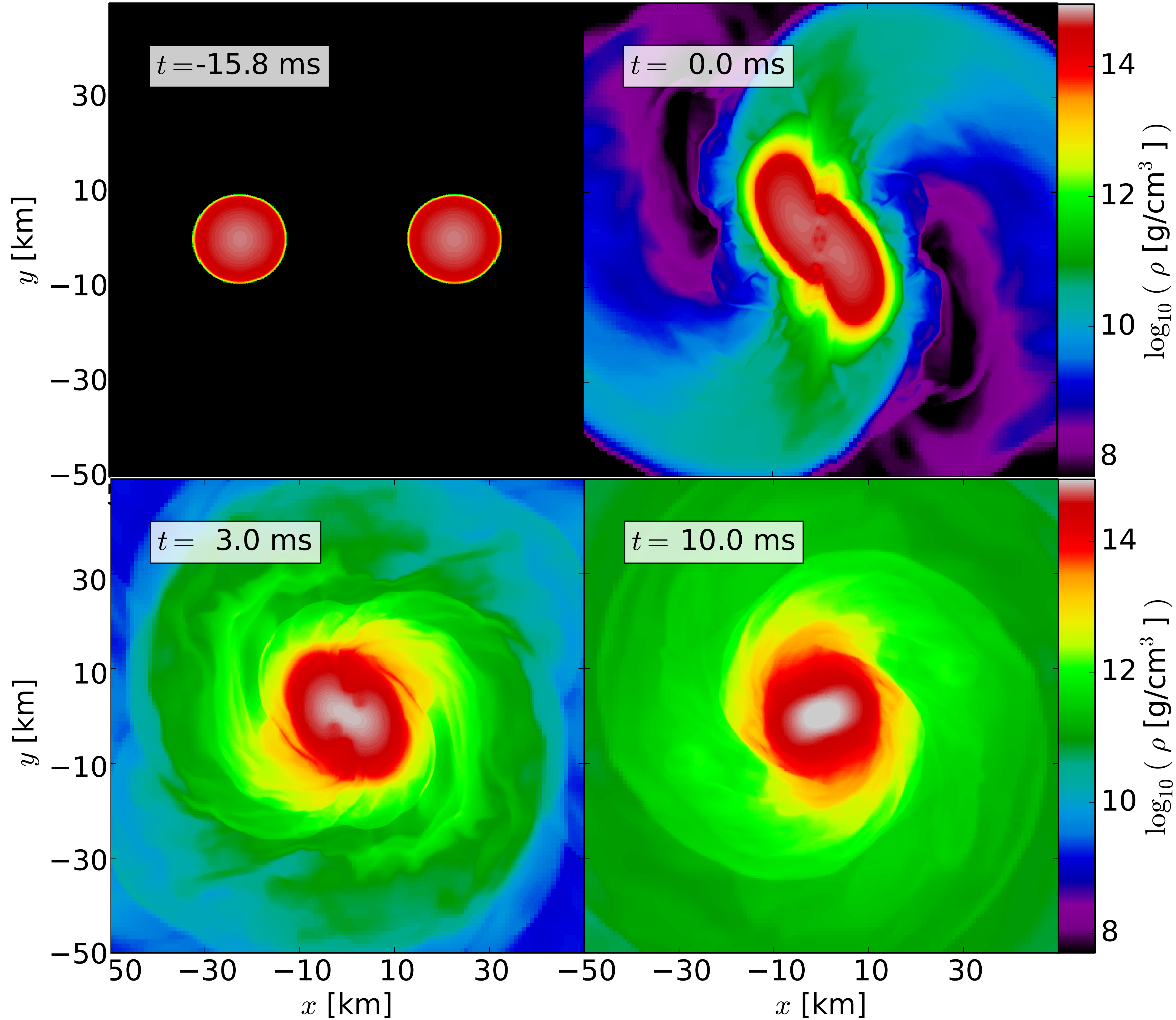


Takami+ 2014

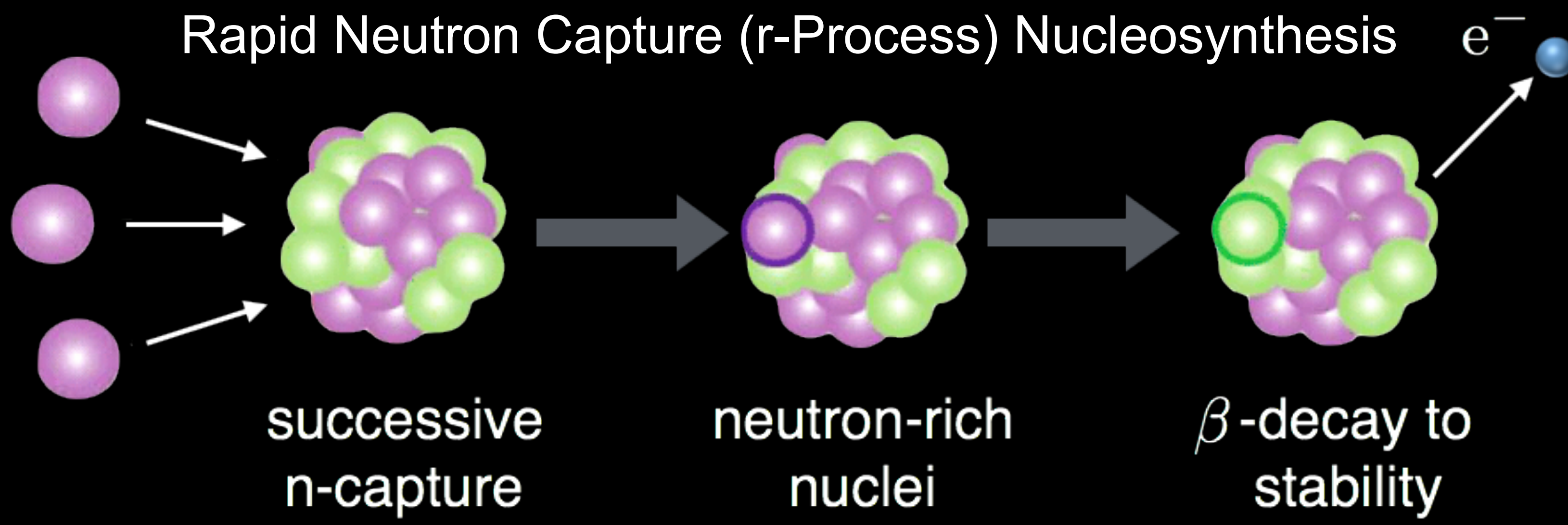


Metzger and Berger, 2012

- binary neutron star mergers are multi-messenger sources
- afterglows are largely driven by production of heavy elements by neutron capture (r-process) and their nuclear decay

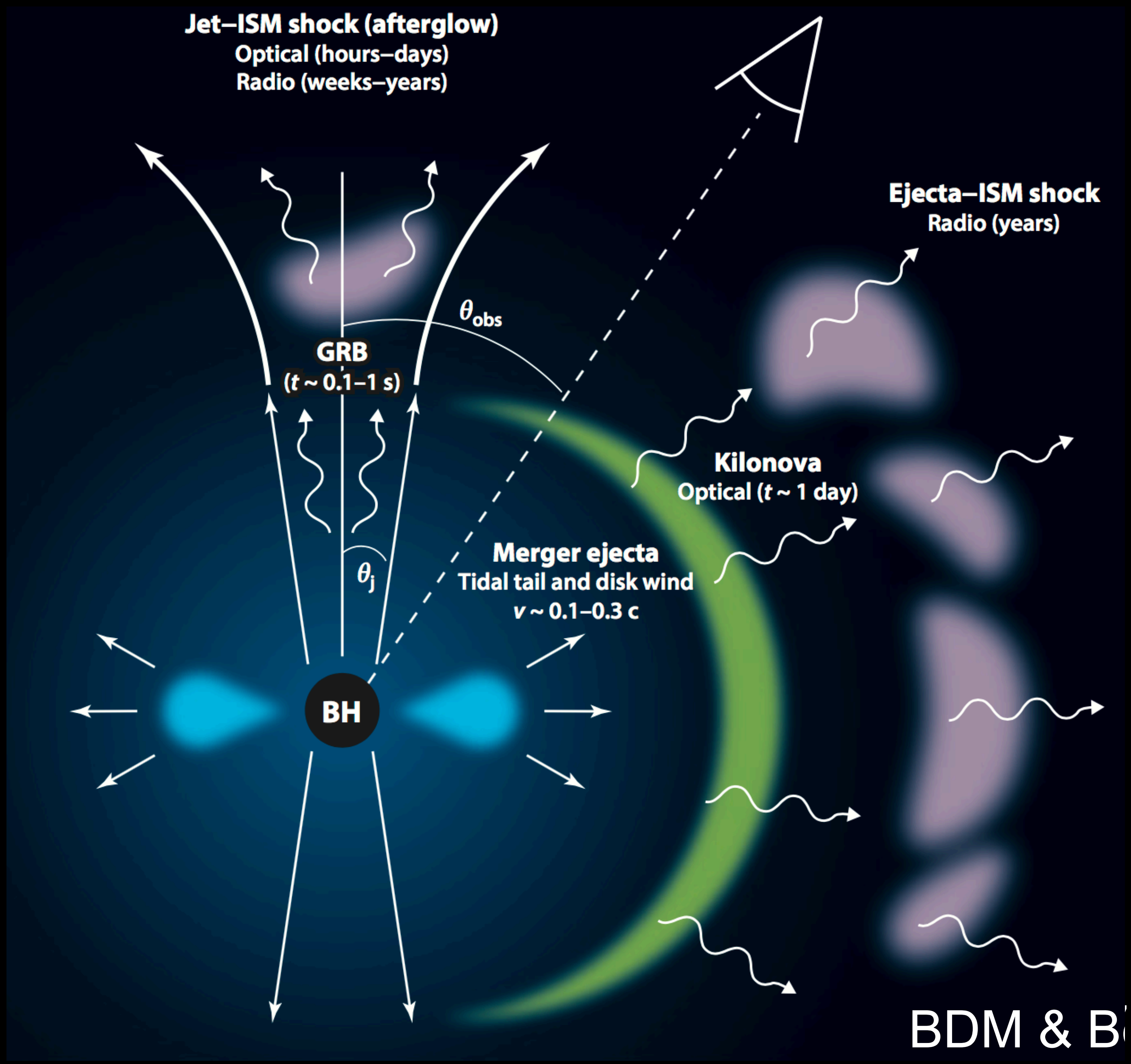

# SPECTRUM OF NEUTRON-STAR BINARIES VIS-A-VIS BLACK HOLE-NEUTRON STAR OR BLACK-HOLE BINARIES

[Bartos, Brady, Marka, CQG **30**, 123001 (2013)]

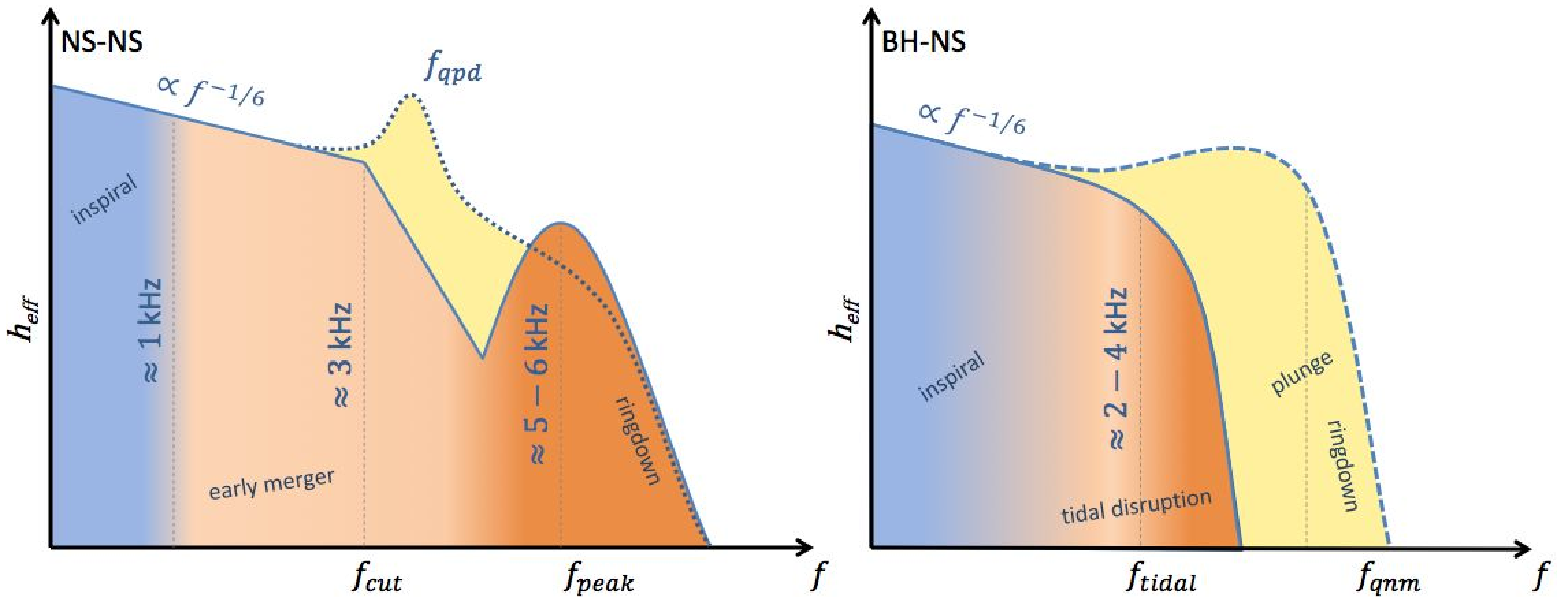

# BINARY NEUTRON STARS: POST-MERGER WAVEFORMS

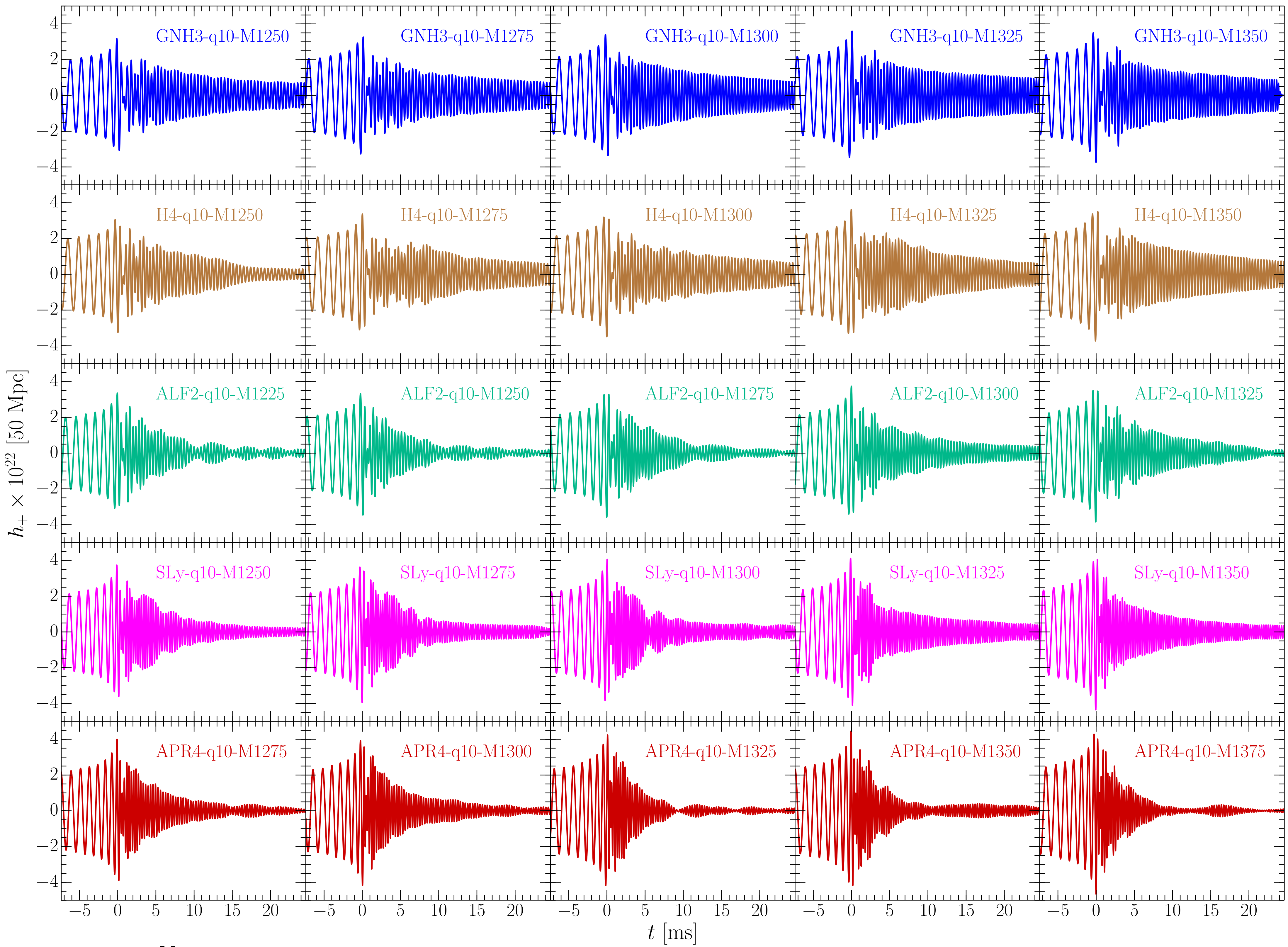


Takami, Rezzolla, Baiotti, 2014

# BINARY NEUTRON STARS: POST-MERGER SPECTRUM

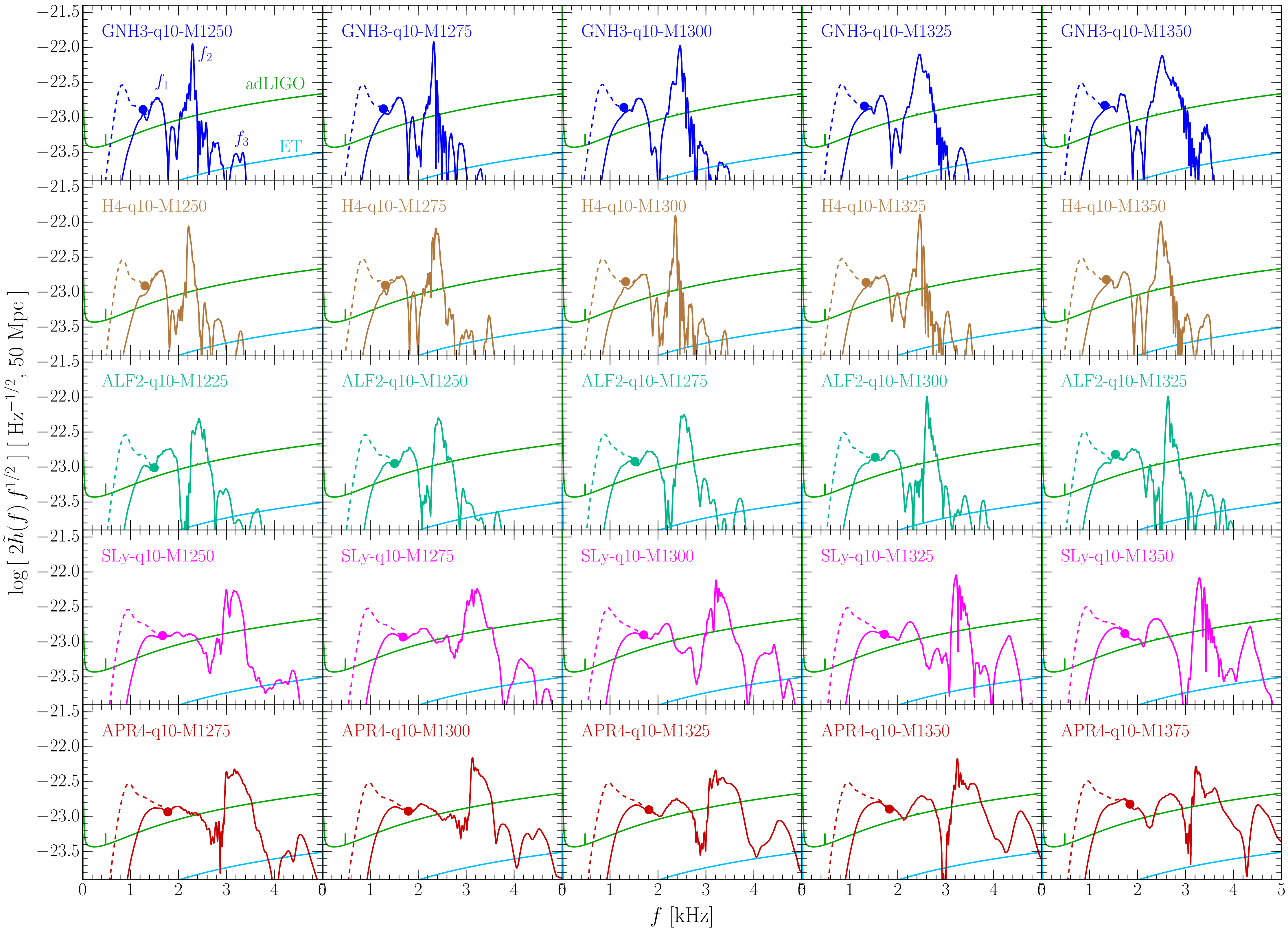


Takami, Rezzolla, Baiotti, 2014

# ANATOMY OF A BINARY NEUTRON STAR COALESCENCE WAVEFORM

early inspiral modeled by post-Newtonian theory - $(v/c)^n$

late inspiral modeled by effective one-body approximation

merger and post-merger oscillations using numerical simulations

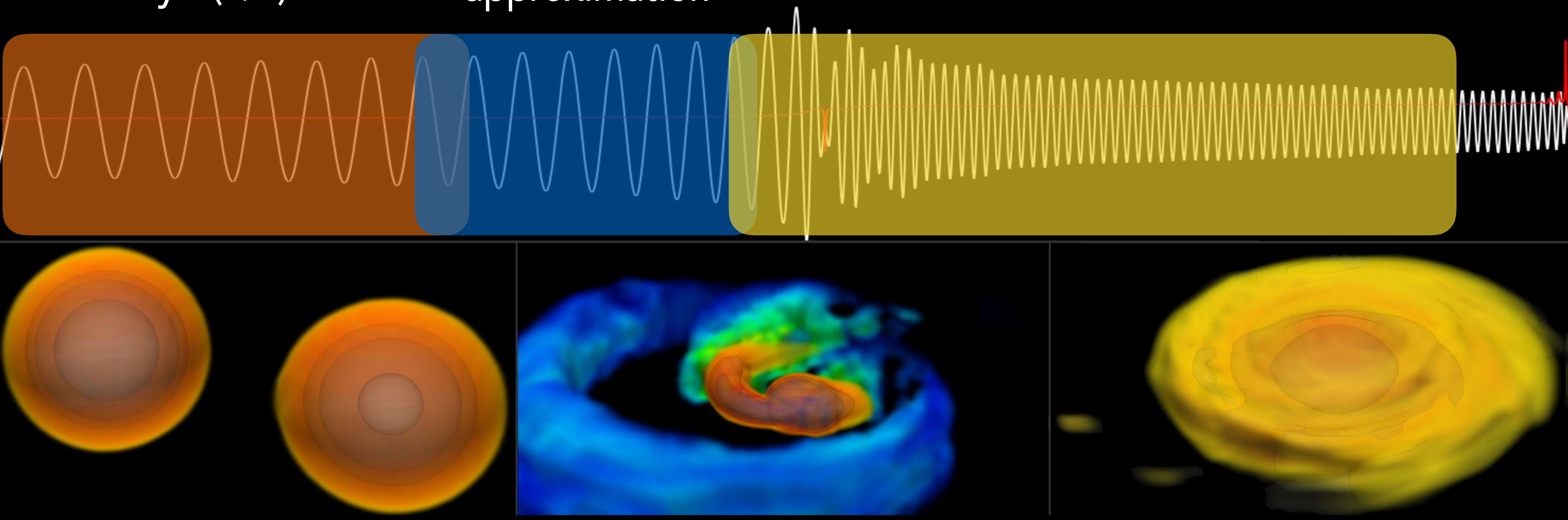

Image: Bernuzzi

# PHYSICAL EFFECTS IN BINARY NEUTRON STAR COALESCENCE WAVEFORMS

dominated by gravitational radiation back reaction - masses and spins

tidal effects appear at high PN order, dynamical tides might be important

complex physics of the merger remnant, multi-messenger source, signature of neutron star EoS

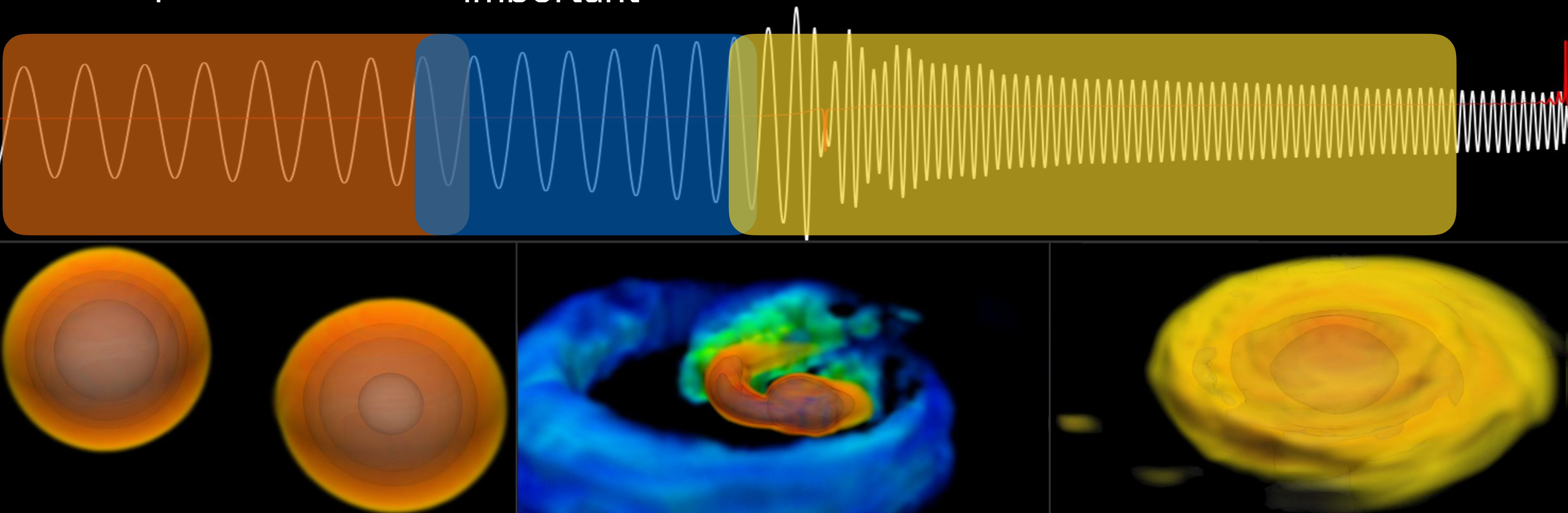

Image: Bernuzzi

# SIGNATURE OF EOS IN BNS WAVEFORMS

- Tidal tensors $\mathcal{E}_{ij}$ of one of the component of the binary induces quadrupole moment $Q_{ij}$ in the other
- variation in the quadrupole moment causes GW emission
- in the adiabatic approximation

$$Q_{ij} = -\lambda(m)\,\mathcal{E}_{ij}, \qquad \lambda(m) = (2/3)\,k_2(m)\,R^5(m)$$

- where $\lambda$(m) is EoS dependent tidal deformability, $k_2$(m) is the Love number and $R$ is the NS radius
- Just from the scaling this is a 5-PN effect $(v/c)^{10}$

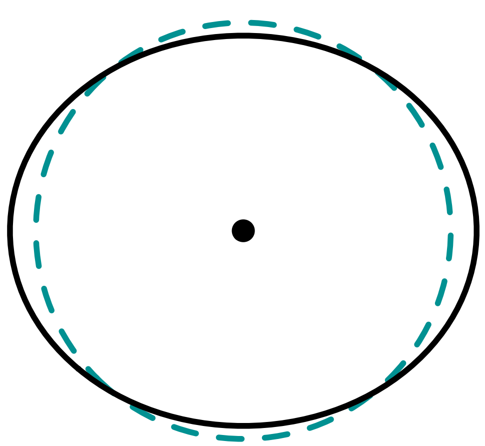

$$\lambda = \frac{Q}{\mathcal{E}} = \frac{\text{size of quadrupole deformation}}{\text{strength of external tidal field}}$$

Tidal deformability

Love number $k_2$

Radius $R$

$$\lambda = \frac{2}{3}k_2R^5 \quad (G = c = 1)$$

$$\Lambda \equiv G\lambda(Gm_{\rm NS}/c^2)^{-5}$$

$$\Lambda \in [300, 600]$$

image: J. Read

# TIDAL TERMS IN THE INSPIRAL REGIME

$$\Psi(v) = \Psi_{\rm PP}(v) + \Psi_{\rm tidal}(v),$$

$$\begin{aligned}\Psi_{\rm tidal}(v) \;=\; & \frac{3}{128\eta} v^{-5} \sum_{A=1}^{2} \frac{\lambda_A}{M^5 X_A} \Big[ -24\,(12 - 11 X_A)\; v^{10} \\ & + \frac{5}{28} \left(3179 - 919 X_A - 2286 X_A^2 + 260 X_A^3\right) v^{12} \\ & + 24\pi (12 - 11 X_A) v^{13} \\ & - 24 \left( \frac{39927845}{508032} - \frac{480043345}{9144576} X_A + \frac{9860575}{127008} X_A^2 \right. \\ & \left. - \frac{421821905}{2286144} X_A^3 + \frac{4359700}{35721} X_A^4 - \frac{10578445}{285768} X_A^5 \right) v^{14} \\ & + \frac{\pi}{28} \left(27719 - 22127 X_A + 7022 X_A^2 - 10232 X_A^3\right) v^{15} \Big]\end{aligned}$$

$$X_A = m_A/M,\; A = 1,2,\; \text{and}\; \lambda_A = \lambda(m_A)$$

plus the quadrupole-monopole interaction

# QUADRUPOLE-MONOPOLE TERM

- Spin-induced deformation leads to quadrupole that depends as spin-square

$$\Psi_{\rm QM}(v) = -\frac{30}{128\eta}\sigma_{\rm QM} v^{-1},$$

$$\begin{aligned}\sigma_{\rm QM} =& -\frac{5}{2}\sum_{A=1,2} q_A \left(\frac{m_A}{M}\right)^2 \left[3(\hat{\chi}_A\cdot\hat{L})^2 - 1\right] \\ \simeq& \frac{5}{2}\sum_{A=1,2} a(m_A)\left(\frac{m_A}{M}\right)^2 \left[3(\hat{\chi}_A\cdot\hat{L})^2 - 1\right]\chi_A^2\end{aligned}$$

$$q \simeq -a\chi^2,$$

$$\mathcal{C} = 0.371 - 3.91\times 10^{-2}\ln\frac{\lambda}{m^5} + 1.056\times 10^{-3}\left(\ln\frac{\lambda}{m^5}\right)^2$$

# WILL THERE BE A PLUNGE PHASE?

$$f_{\rm LSO} = \frac{1}{6^{3/2}\pi M}.$$

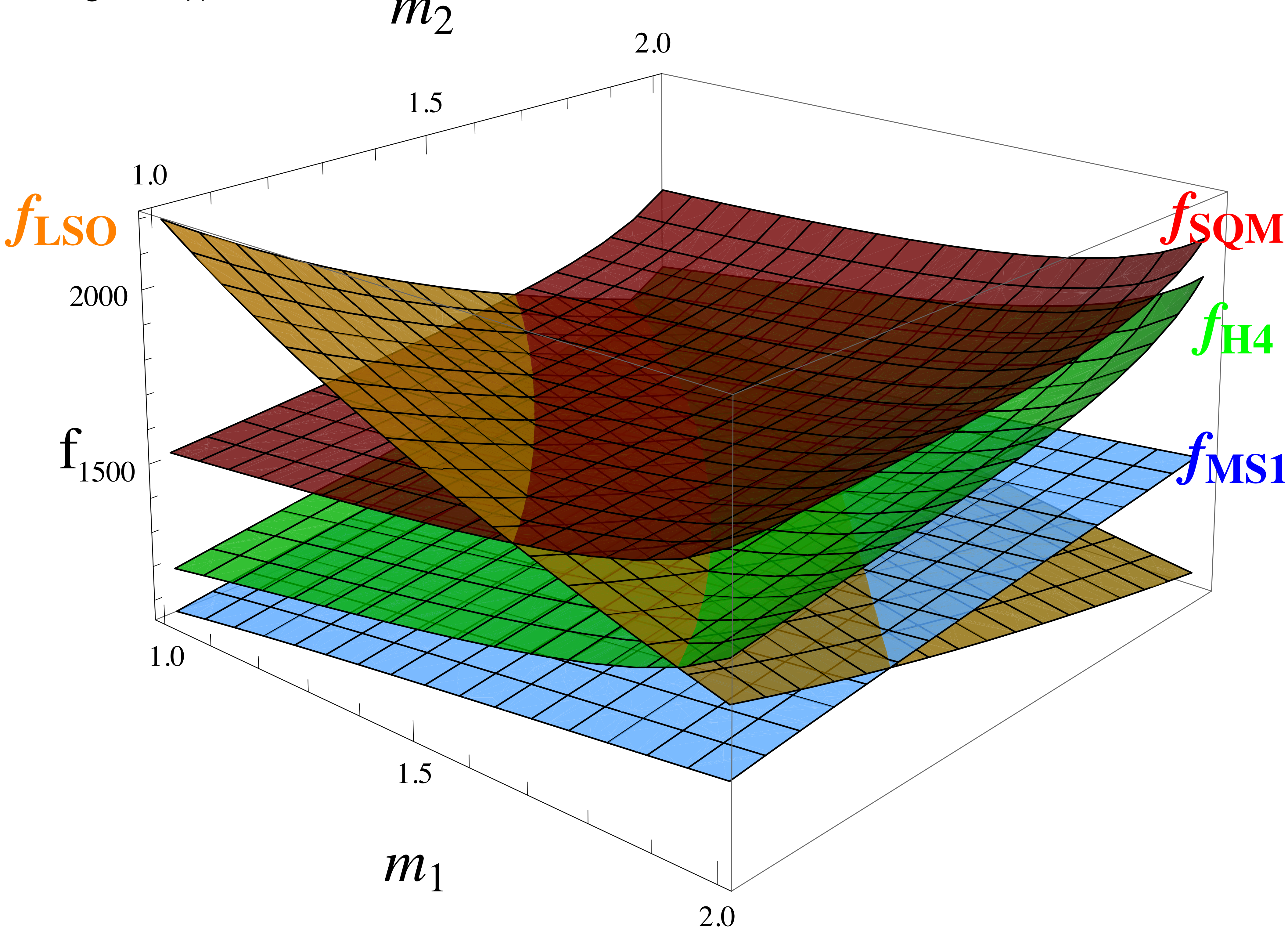


Agathos+, 2015

# ACCURATE WAVEFORM MODELS IS KEY TO GW MEASUREMENT OF NS RADIUS

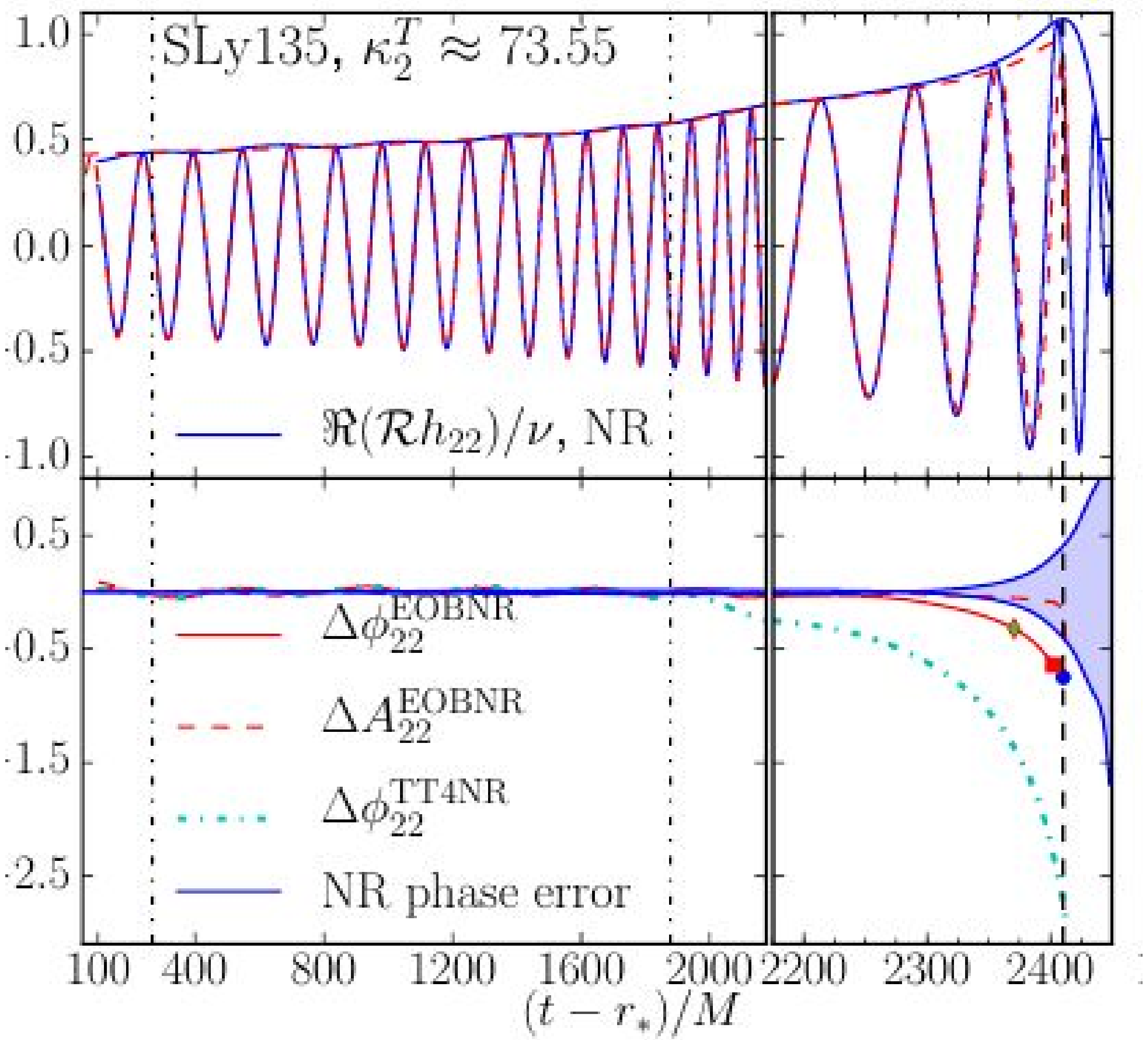


[Bernuzzi+, PRL **115**, 091101 (2015)]

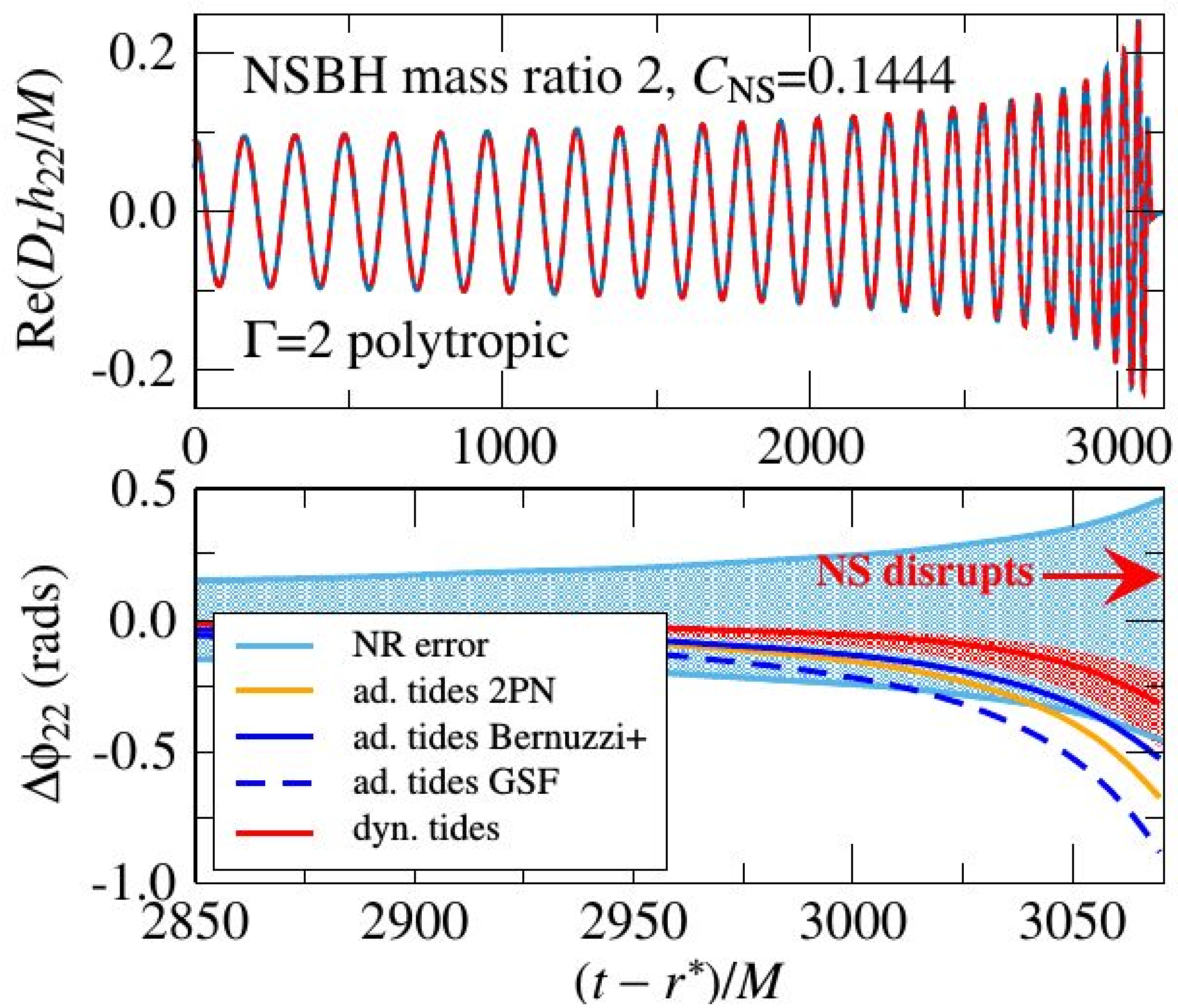


[Hinderer+, PRL **116**, 181101 (2016)]

# EOS USED IN AGATHOS+ PAPER

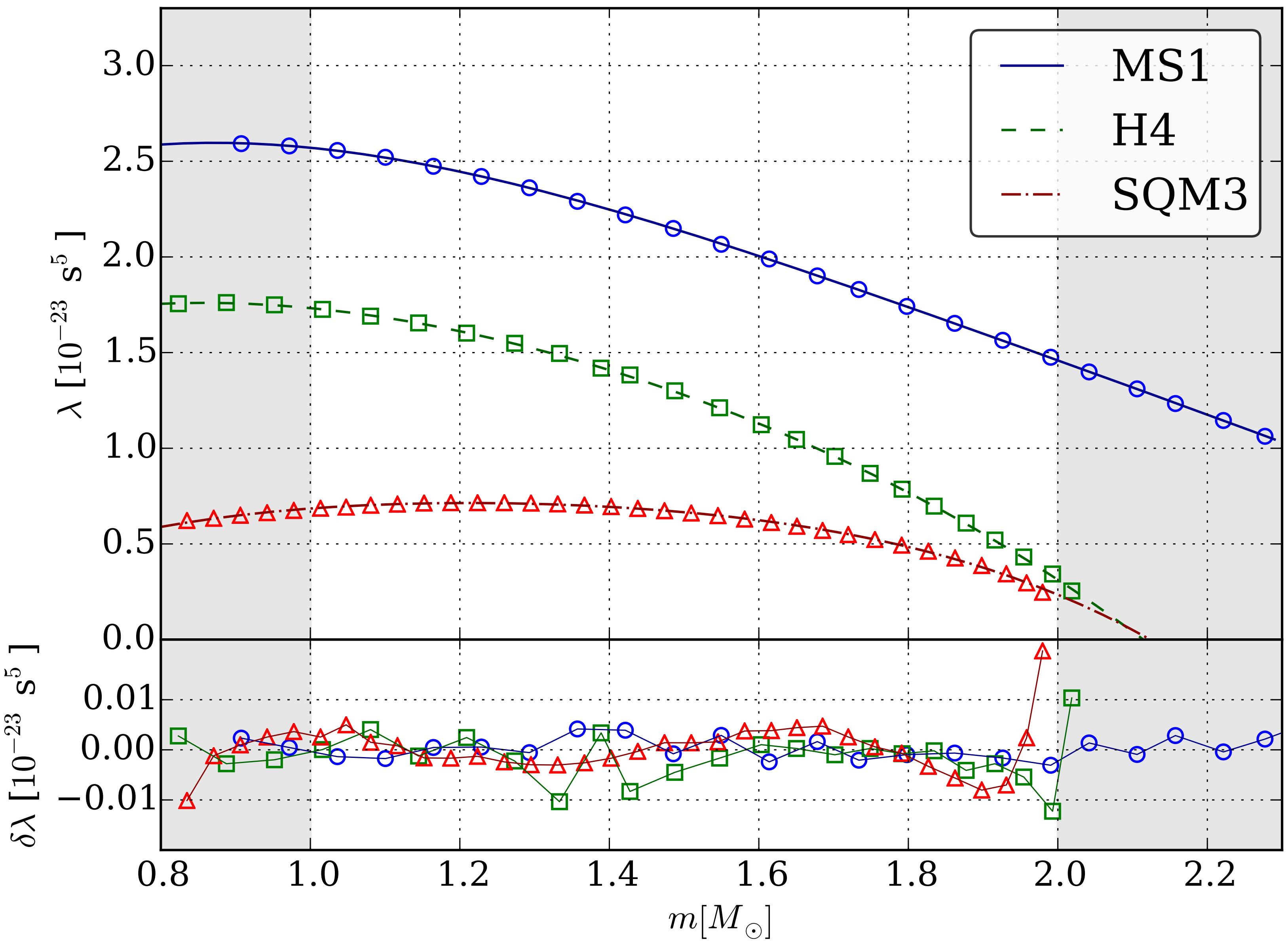


The tidal deformability parameter λ(m) as a function of neutron star mass for three different EOS: a soft one (SQM3), a moderate one (H4), and a stiff one (MS1). Adapted from [18]. Curves are fitted quartic polynomials, whose residuals are shown in the lower subplot. Only masses within the unshaded region [1, 2]M⊙ will be considered in our analyses.

# STATISTICAL AND SYSTEMATIC ERRORS ON C0

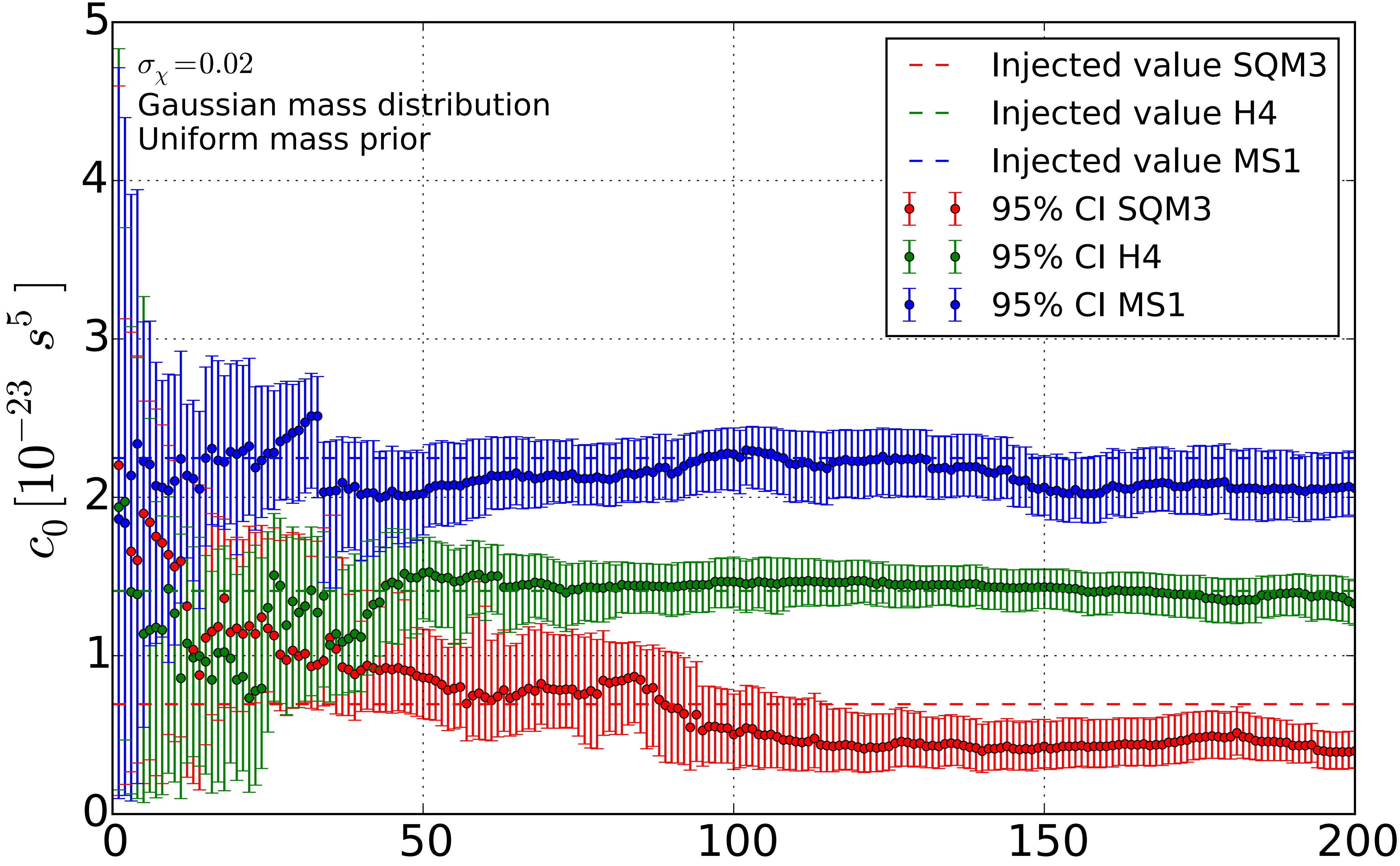


Agathos+, 2015

# NS EQUATION OF STATE

*INCLUDING THE POST-MERGER PHASE*

# MODELING BNS WAVEFORM BEYOND INSPIRAL

- Develop analytical time-domain fits of post-merger waveforms and combine them with those of pre-merger waveforms.
- Use these waveforms to estimate errors in BNS parameters, including NS EOS parameters.

# BINARY NEUTRON STAR WAVEFORMS

$$h(t) = \alpha \exp(-t/\tau_1)\left[\sin(2\pi f_1 t) + \sin(2\pi(f_1 - f_{1\epsilon})t) + \sin(2\pi(f_1 + f_{1\epsilon})t)\right] + \exp(-t/\tau_2)\sin(2\pi f_2 t + 2\pi\gamma_2 t^2 + \pi\beta_2).$$

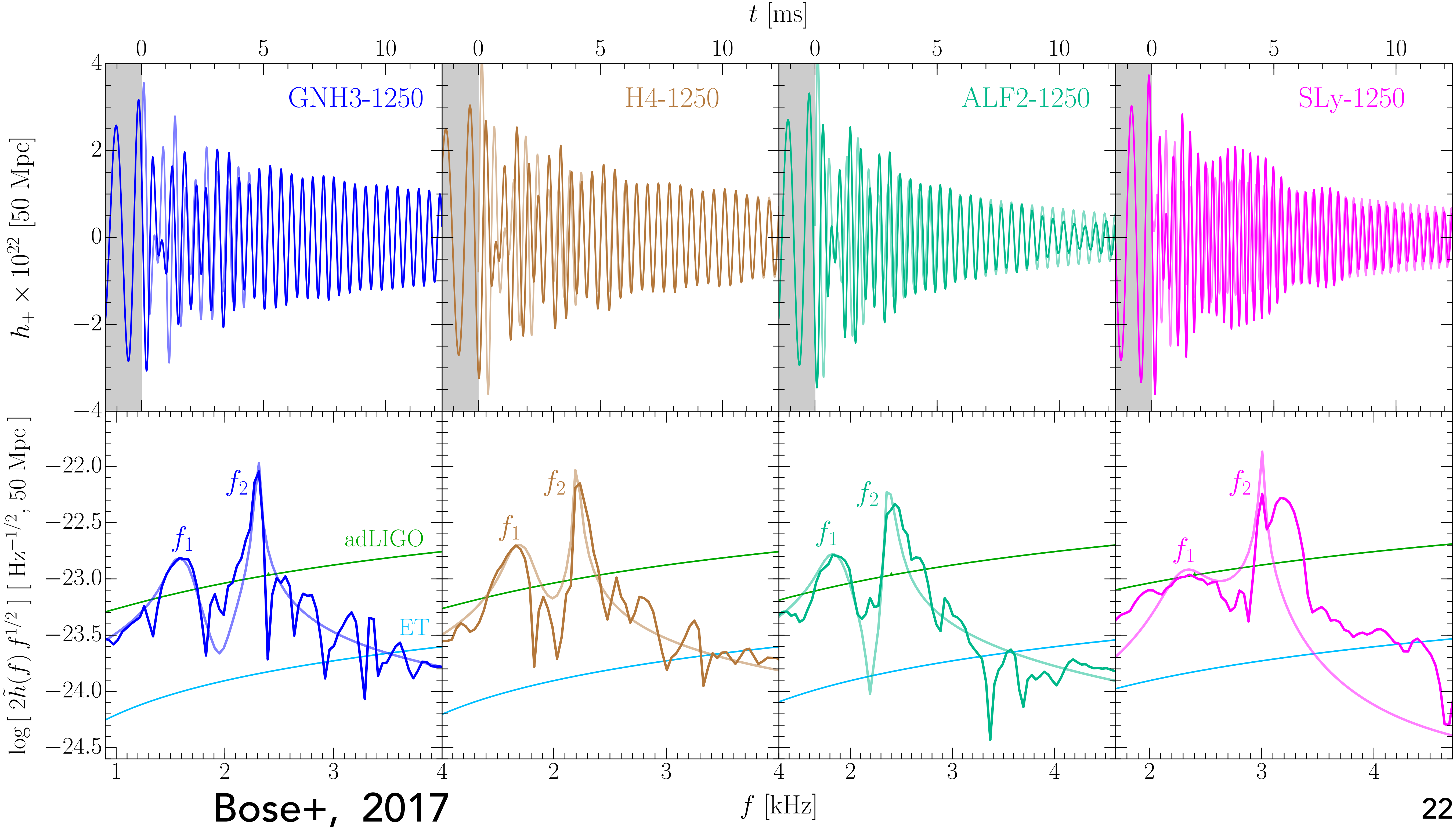


Bose+, 2017

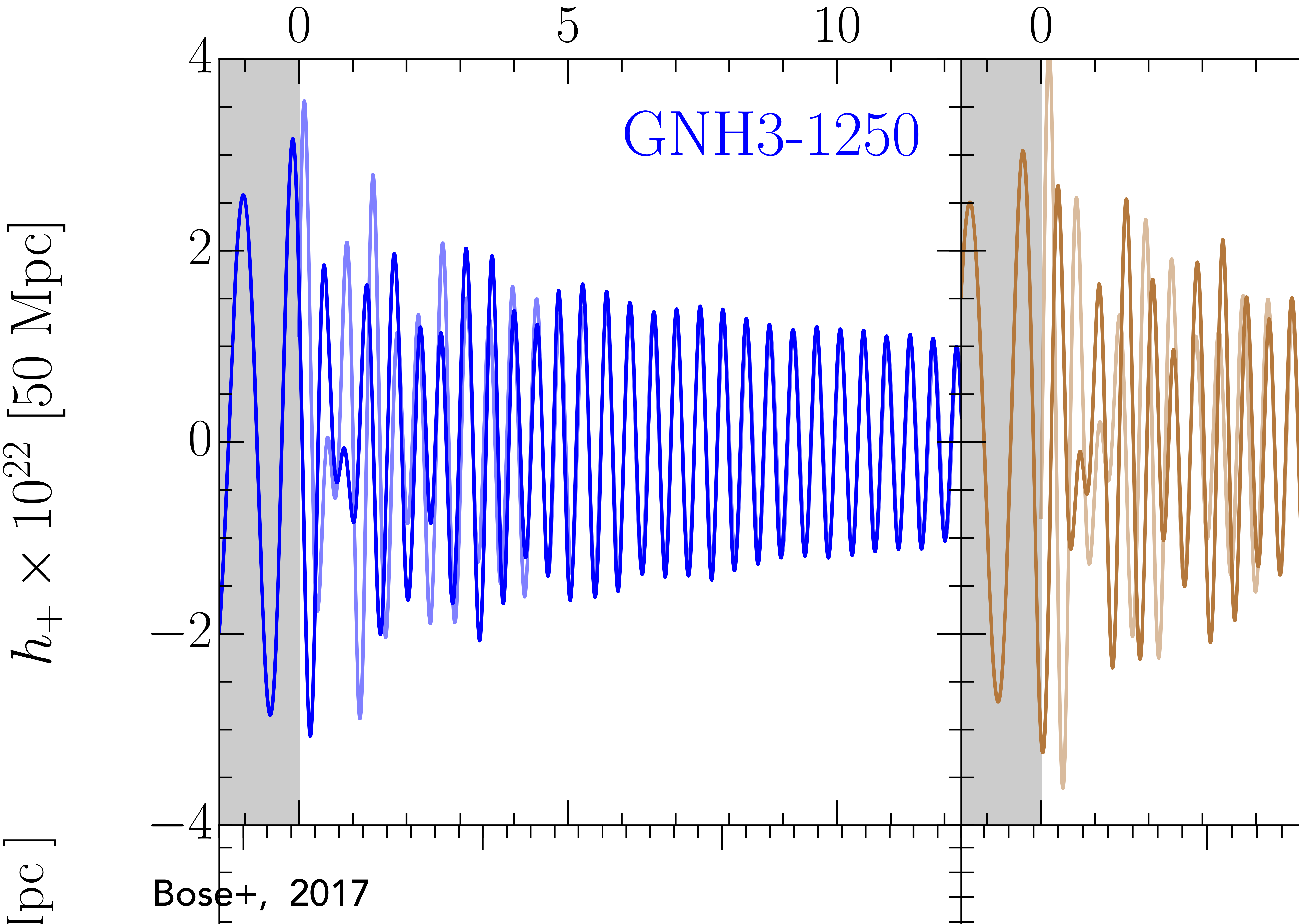


Bose+, 2017

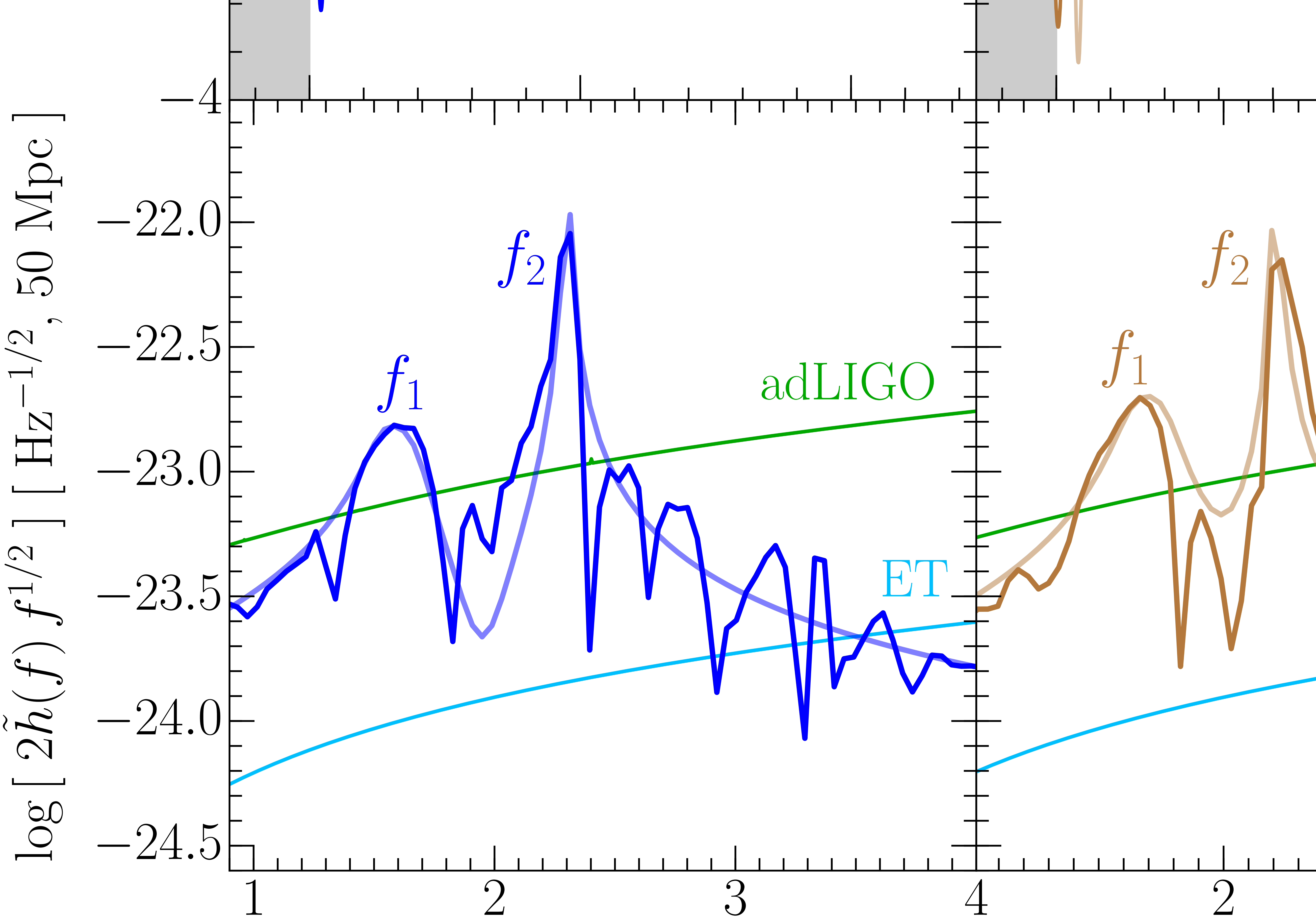

$\log[\,2\tilde{h}(f)\,f^{1/2}\,]\;[\,\mathrm{Hz}^{-1/2},\,50\ \mathrm{Mpc}\,]$
−4
−22.0
−22.5
−23.0
−23.5
−24.0
−24.5
$f_1$
$f_2$
adLIGO
ET
1
2
3
4
2
$f_1$
$f_2$


Bose+, 2017

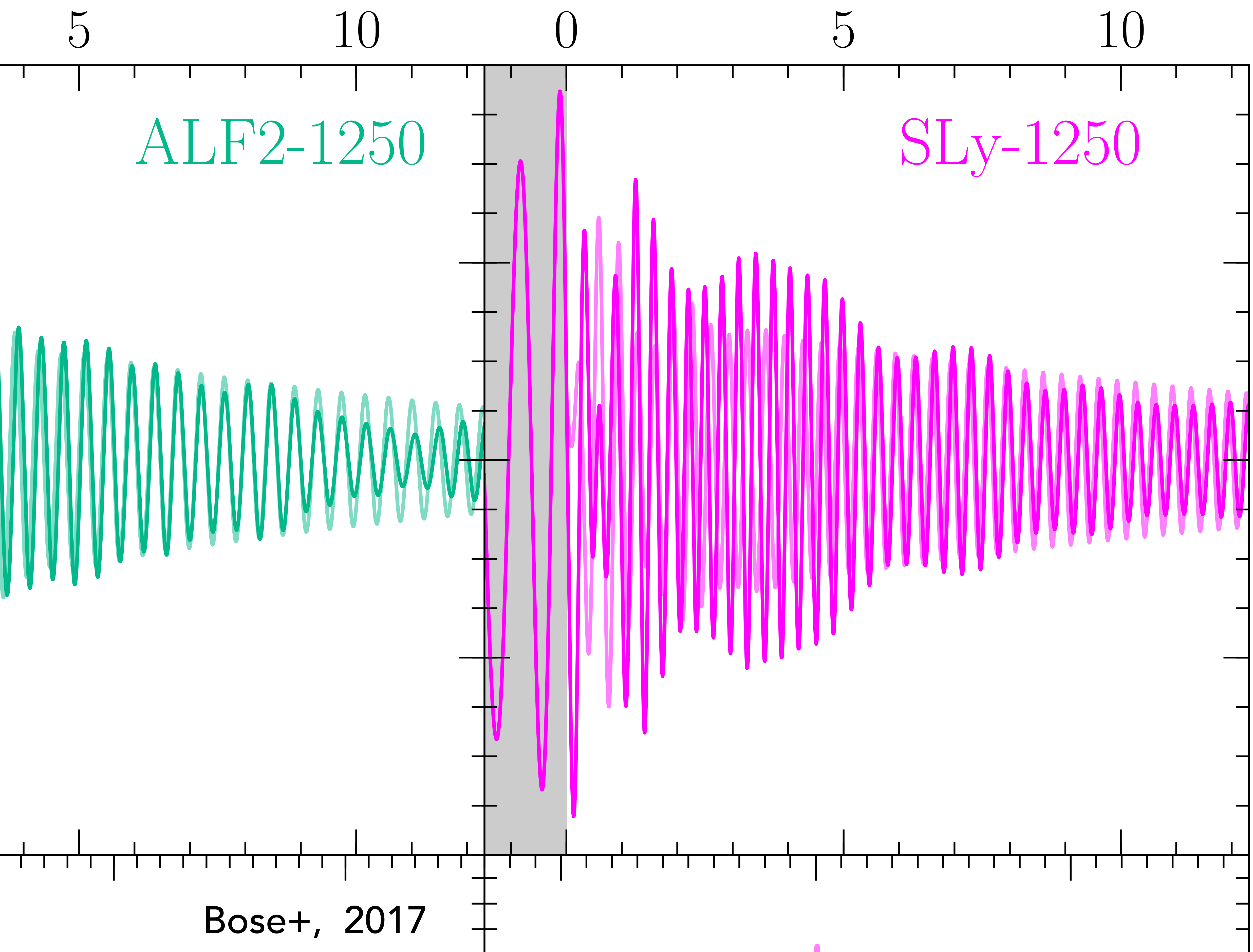


Bose+, 2017

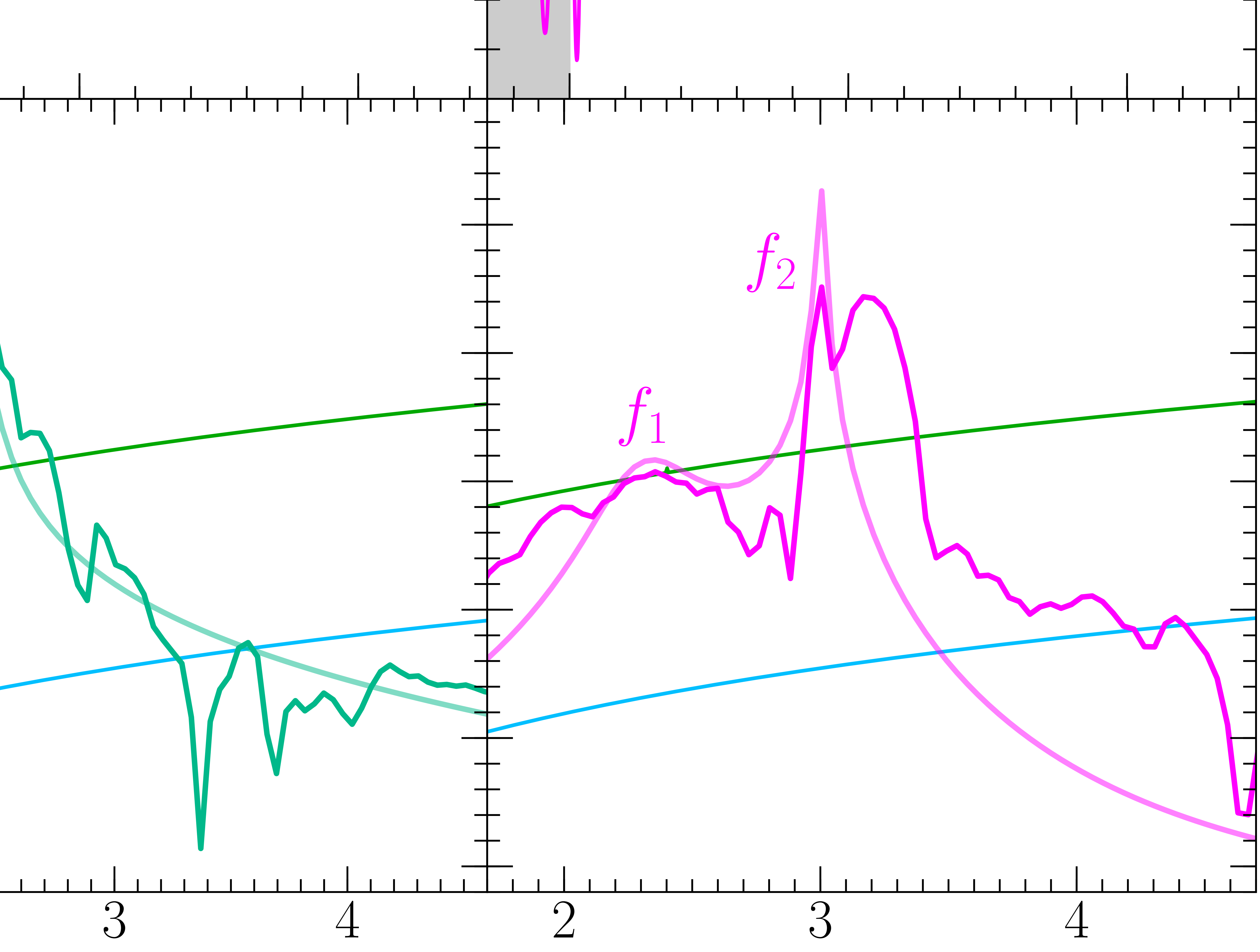


Bose+, 2017

# SCALING RELATIONS: POST MERGER

$$f_1 \approx a_0 + a_1\,\mathcal{C} + a_2\,\mathcal{C}^2 + a_3\,\mathcal{C}^3 \text{ kHz},$$

$$f_2 \approx b_0 + b_1\,\mathcal{C} + b_2\,\mathcal{C}^2 \text{ kHz},$$

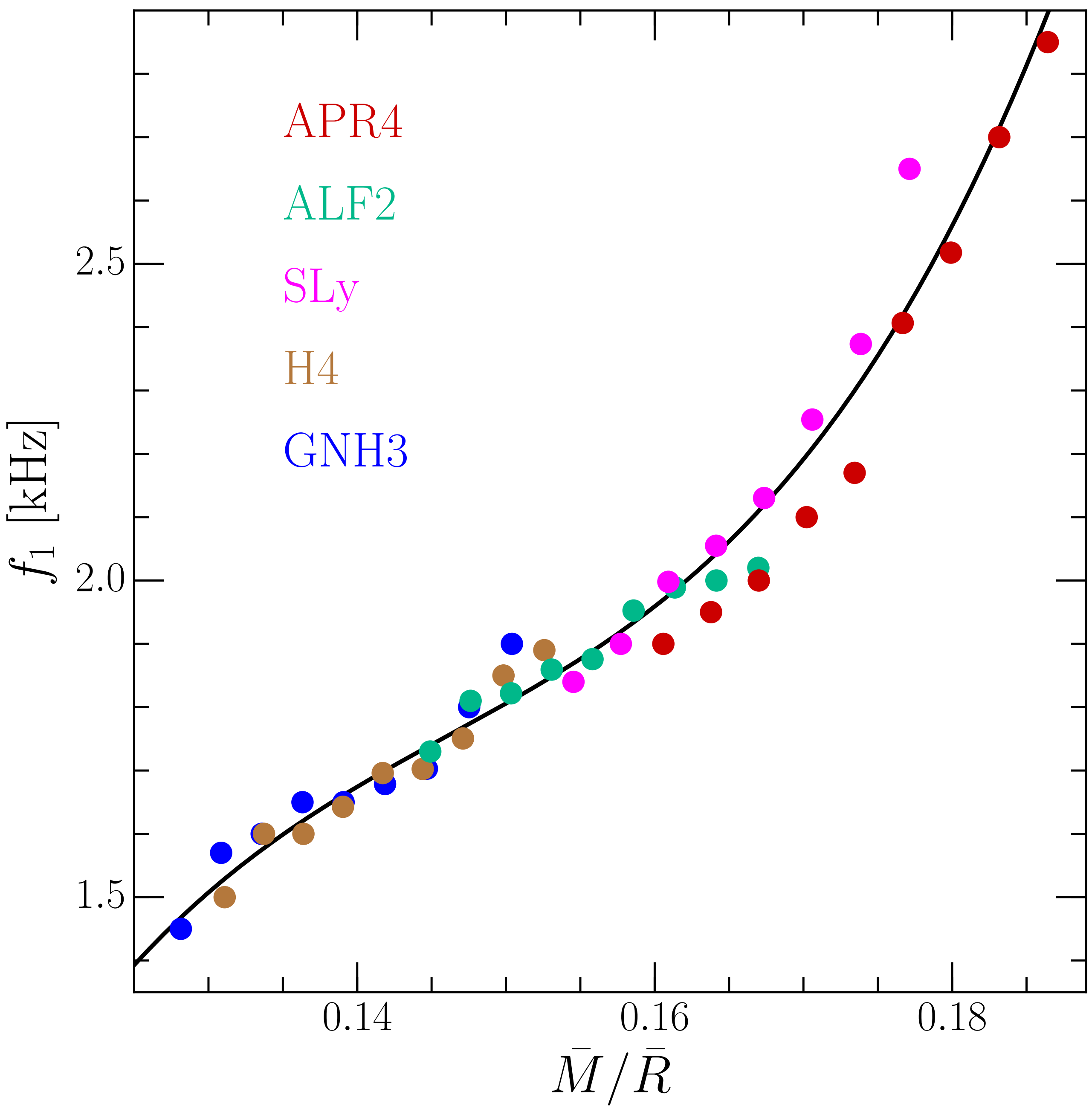


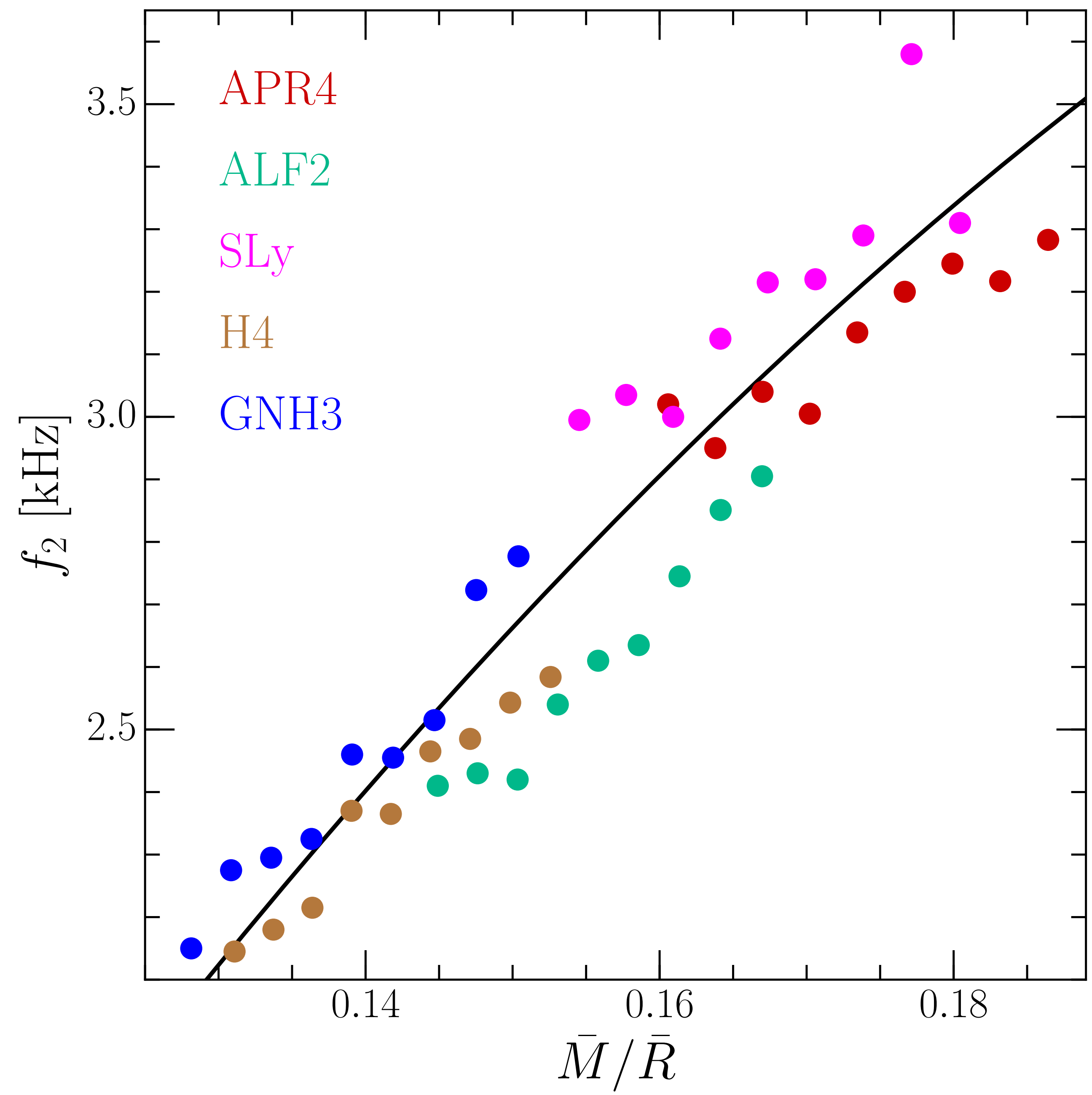


Bose+, 2017

# SCALING RELATIONS: POST MERGER

$$f_1 \approx c_0 + c_1 x + c_2 x^2 + c_3 x^3 \text{ kHz}$$

$$x = (\kappa_2^T)^{1/5} \qquad f_2 \approx 5.832 - 1.118x \text{ kHz}$$

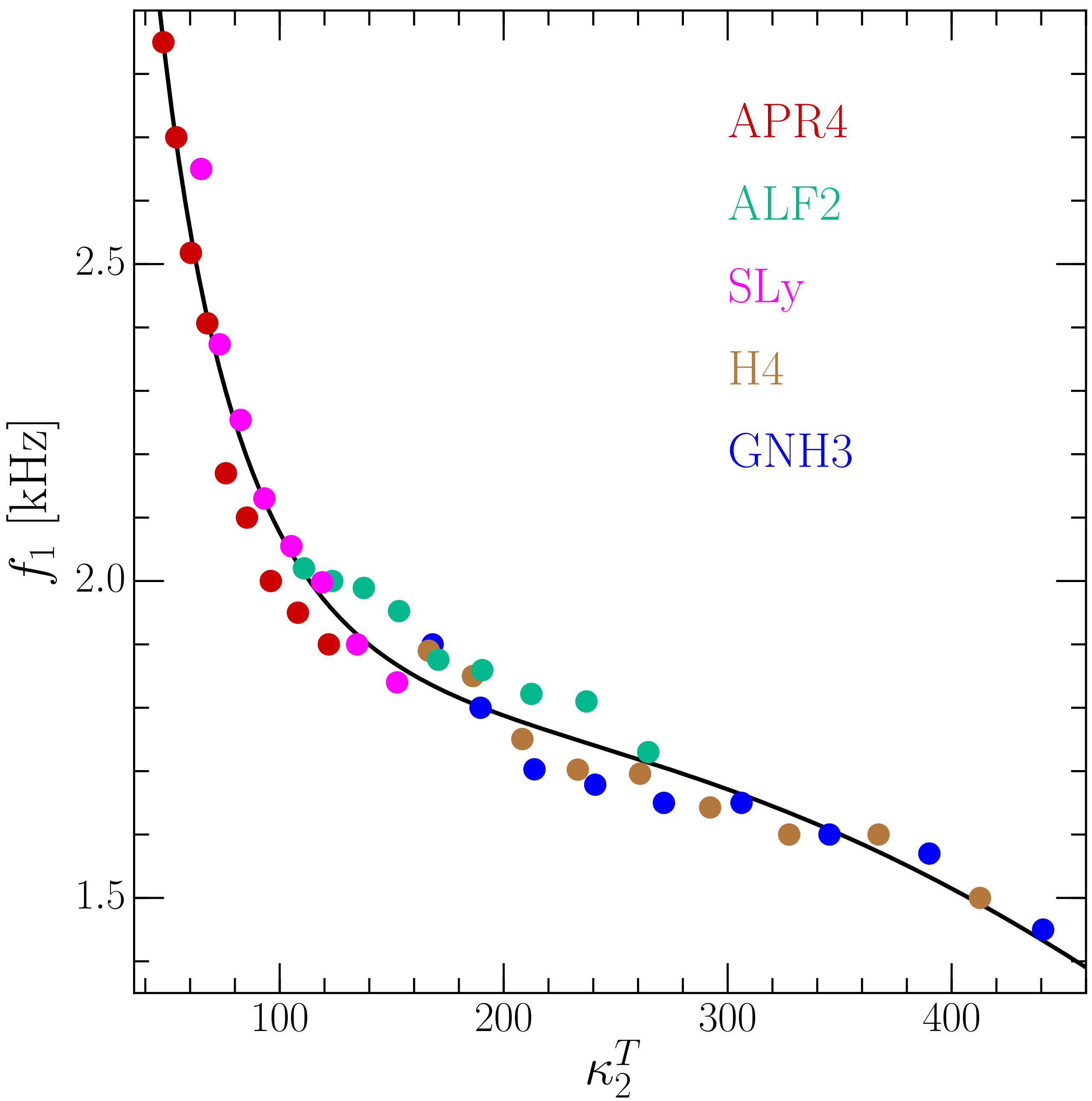


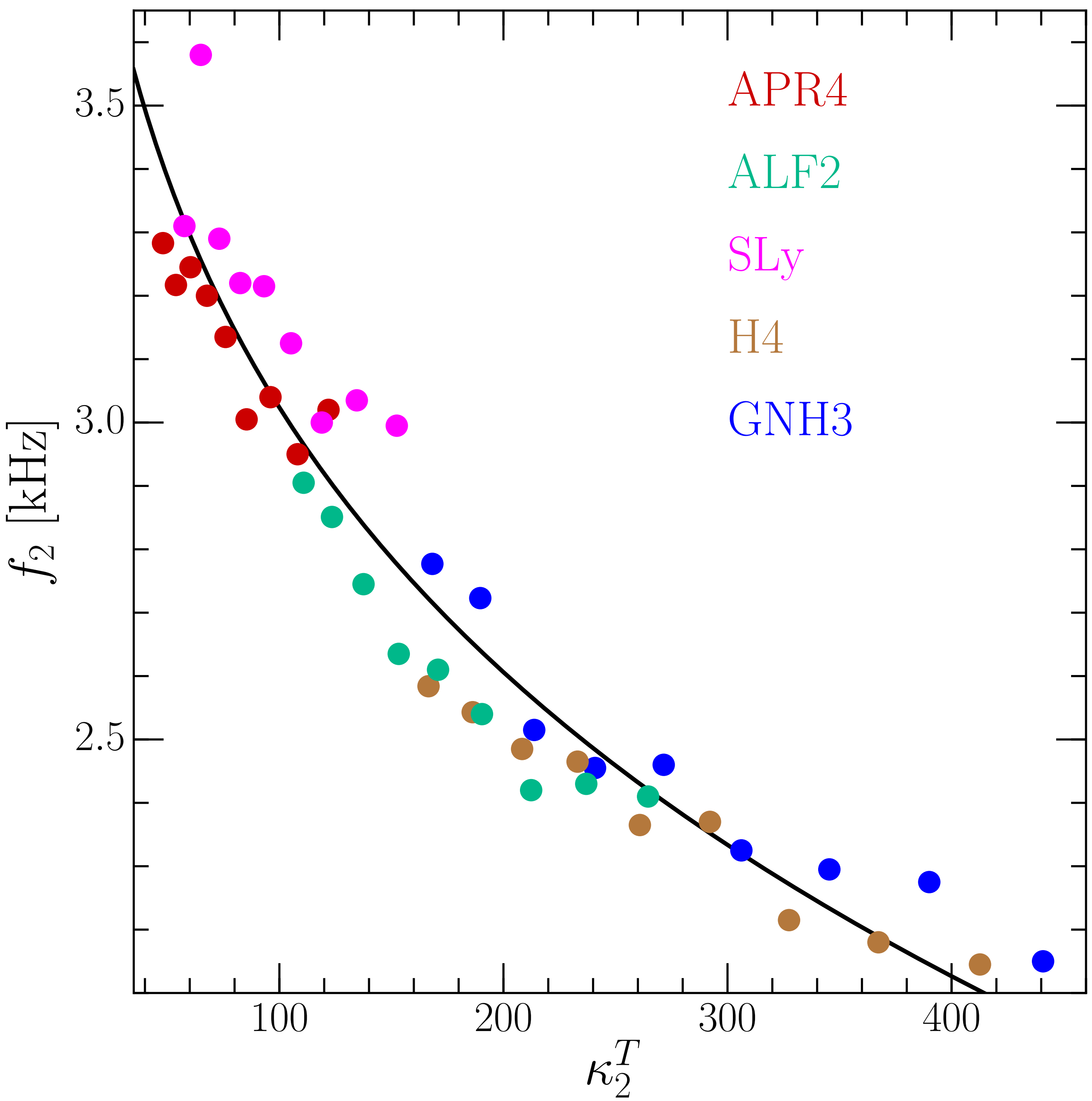


Bose+, 2017

# SCALING RELATIONS

$$\log_{10}(\kappa_2^T) \simeq d_0 + d_1\,\mathcal{C} + d_2\,\mathcal{C}^2 + d_3\,\mathcal{C}^3\,,$$

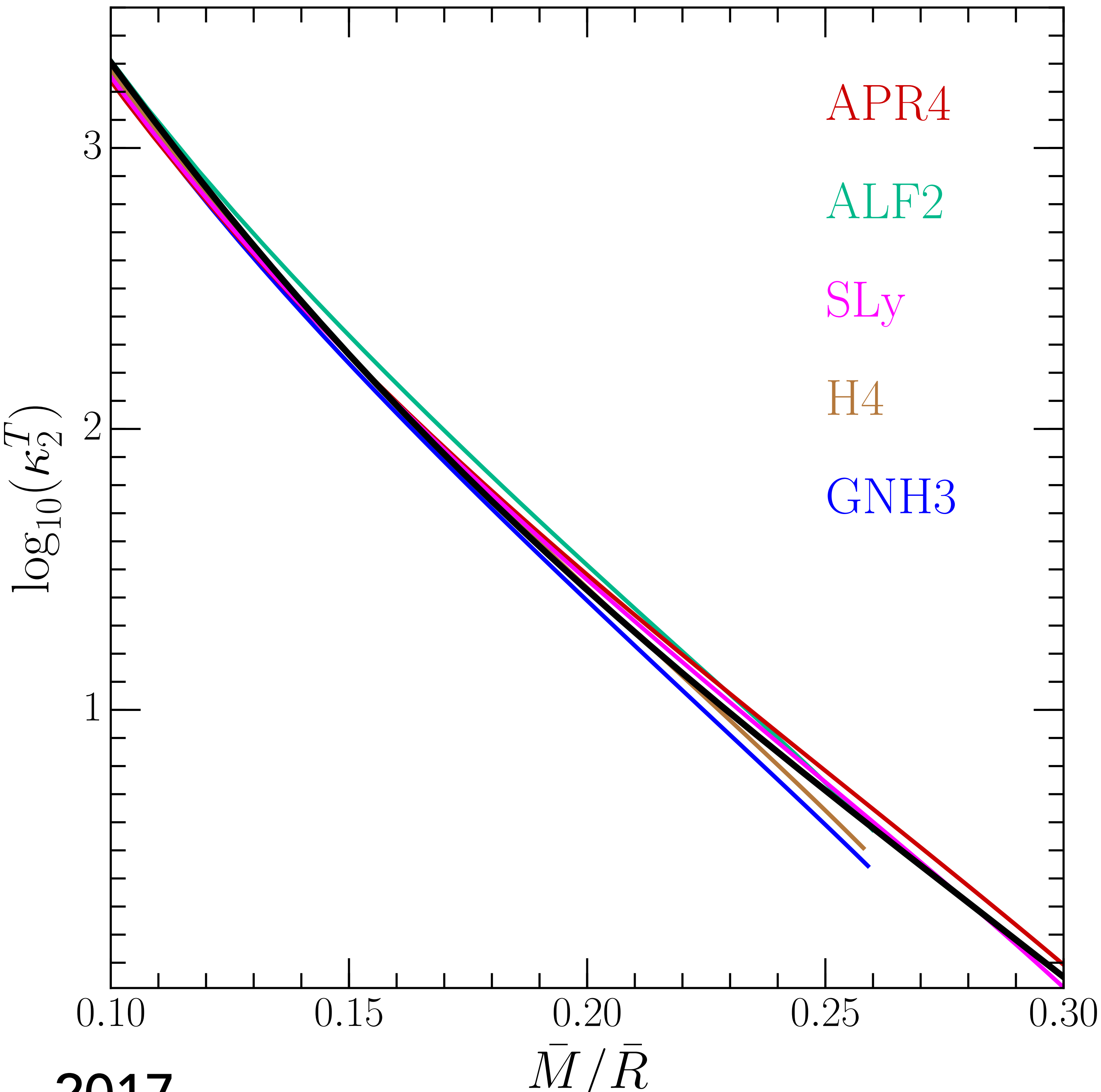


Bose+, 2017

# MEASUREMENT ACCURACY OF COMPACTNESS

| binary | $f_1$ [kHz] | $\tau_1$ [ms] | $f_2$ [kHz] | $\tau_2$ [ms] | $\gamma_2$ [$Hz^2$] | $\xi_2$ [$Hz^3$] | $\alpha$ | $\Delta f_1$ [Hz] | $\Delta f_2$ [Hz] | $\Delta\mathcal{C}/\mathcal{C}$ [%] | $\Delta f_2^{\rm MC}$ [Hz] | $[\Delta R/R]^{\rm MC}$ [%] |
|---|---|---|---|---|---|---|---|---|---|---|---|---|
| GNH3-1250 | 1.60 | 2 | 2.30 | 23.45 | 38 | -9.e2 | 0.46 | 371 | 29 | 1.0 | 14.3 | 1.8 |
| H4-1250 | 1.65 | 5 | 2.22 | 20.45 | -677 | 0.0 | 0.55 | 151 | 43 | 1.2 | 50 | 2.7 |
| ALF2-1250 | 1.85 | 15 | 2.42 | 10.37 | -3467 | 2.e4 | 0.55 | 66 | 133 | 3.4 | 62.5 | 3.0 |
| SLy-1250 | 2.30 | 1 | 3.00 | 13.59 | 0 | 0.0 | 0.50 | 1683 | 82 | 2.2 | 52.0 | 2.4 |
| GNH3-1325 | 1.70 | 2 | 2.45 | 23.45 | 342 | 5.e4 | 0.35 | 371 | 40 | 1.0 | 100 | 4.5 |
| H4-1325 | 1.75 | 5 | 2.47 | 20.45 | -1077 | 4.5e3 | 0.30 | 177 | 27 | 1.0 | 50 | 2.7 |
| ALF2-1325 | 2.05 | 15 | 2.64 | 10.37 | -863 | 2.5e4 | 0.50 | 79 | 60 | 1.6 | 97 | 4.0 |
| SLy-1325 | 2.30 | 1 | 3.22 | 13.59 | -617 | 5.5e4 | 0.50 | 1137 | 74 | 2.0 | 312 | 9.8 |

- Above: Statistical error estimates of f_2, and the compactness C deduced from it, for 100 post-merger systems distributed uniformly in aLIGO volume, with an average distance of 200 Mpc and SNR of 8.
- If component masses can be determined to an accuracy of 10 - 20% from the inspiral phase, then the above compactness errors imply that the radius will be measured to an accuracy of ~10-20%. (But this is a loose statement since masses and radii will vary among the 100 sources.)
- CAVEAT: At the moment systematic errors between post-merger waveforms from different NR groups can be as high as ~10% in estimating the compactness. (Compare this to a few percent statistical error listed in the table above, arising from detector noise.)

Bose+, 2017

# NEUTRON STAR RADIUS MEASUREMENT ACCURACY

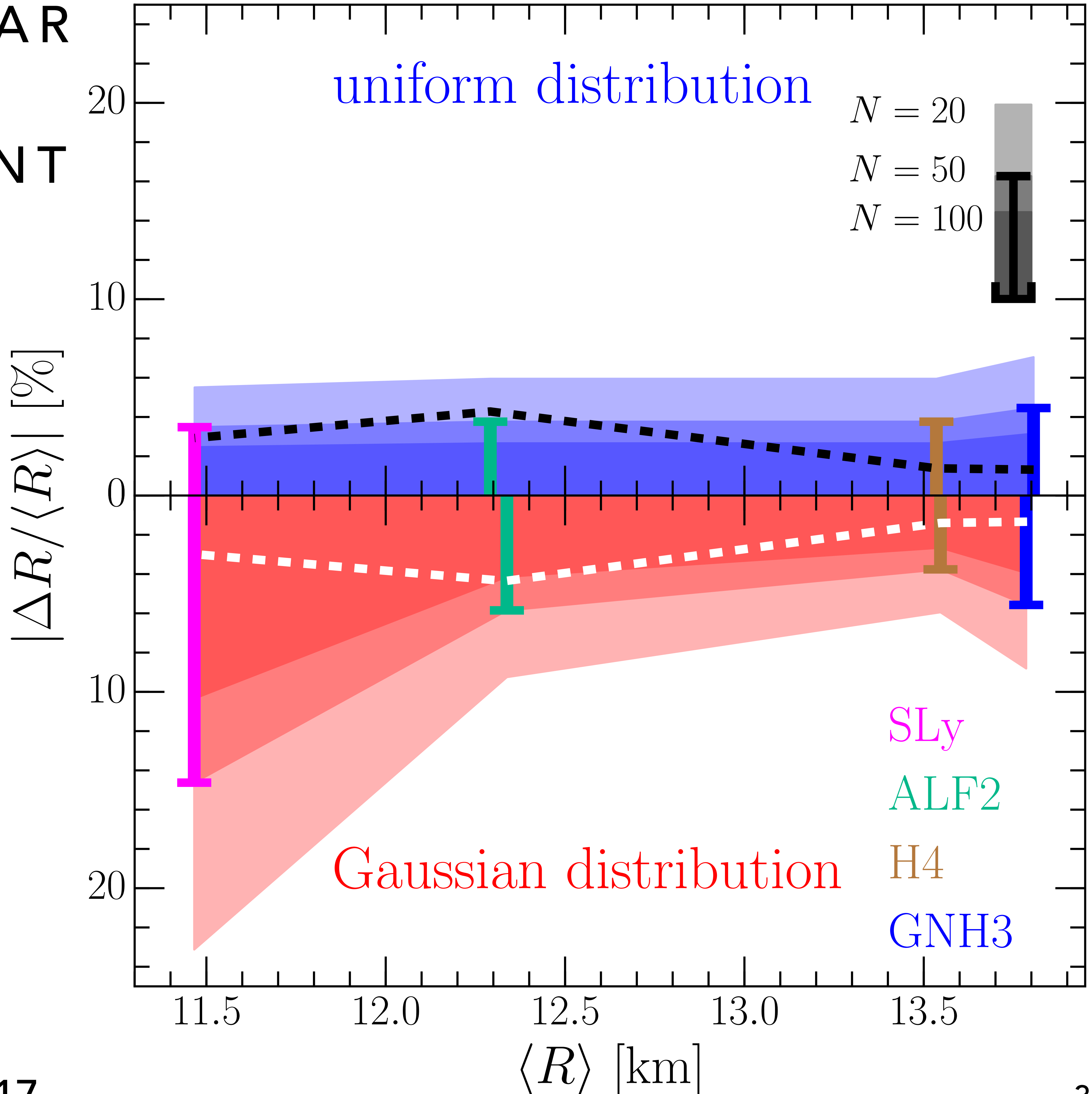


Bose+, 2017

# SUMMARY

- binary neutron star signals are to GW observations as atomic spectra are to EM observations
  - signature of nuclear equation of state is imprinted in the inspiral and post-merger signal
  - GW amplitude gives us distance and spectra could give us redshift
- measuring the NS-EoS and radius via GW observations will take sometime
  - lack of accurate waveform models and systematic biases
  - unknown distribution of neutron star masses and spins
  - insufficient sensitivity at frequencies beyond ~ 500 Hz
  - difficulties with calibration of phase and amplitude of the data
- third generation detectors, and probably new ideas, are needed to impact microphysics from GW observations